MEDICAL UNIVERSITY – VARNA
PROF. DR. PARASKEV STOYANOV
FACULTY OF DENTAL MEDICINE
DEPARTAMENT OF PERIODONTOLOGY AND DENTAL IMPLANTOLOGY

Desislava Kirilova Stoyanova, DMD

Maxillary sinus floor elevation with lateral approach – imaging, clinical and experimental research

THESIS SUMMARY

RESEARCH SUPERVISOR:
Prof. Dr. Stefan Peev, DMD, PhD, DSc
Assoc. Prof. Nikolay Rumenov Sapundziev, MD, PhD

VARNA 2022

The thesis contains 136 pages, 23 tables, 44 figures and 6 appendices. 180 literary sources are cited, of which 5 are in Cyrillic and 175 are in Latin.

The official defense of the thesis will take place on 09.12.2022. in the Auditorium "Assoc. Dr. Dimitar Klisarov" at the Faculty of Dental Medicine at the Medical University" - Varna "Prof. Dr. Paraskev Stoyanov, in a meeting of the scientific jury.

Note: In the thesis, the numbers of the tables and figures do not correspond to those in the thesis summary.

CONTENTS :

ABBREVIATIONS USED

CBCT - Cone beam computed tomography
FDI - Fédération Dentaire Internationale
FDM - Fused Deposition Modeling
FOV - Field of view
M - molar
MS - maxillary sinus
MSFALA - maxillary sinus floor augmentation procedure with lateral approach
MSFALADIP - maxillary sinus floor augmentation procedure with lateral approach with delayed implant placement
MSFALAIIP - maxillary sinus floor augmentation procedure with lateral approach with immediate implant placement
MSW - maxillary sinus width
OPG - orthopantomography
PM - premolar
SBH - subantral bone height
SBW - subantral bone width
SLA - Stereolithography
SLS - Selective laser sintering
STL - Standard Tessellation Language
WHO - World Health Organization

1. INTRODUCTION

In modern dentistry, dental implantology occupies an important place and is increasingly widely advocated, appearing as the optimal option for restoring the masticatory apparatus in case of partial and total edentulism and the only option for non-removable/permanent prosthetics in case of distally unlimited defects of the dental rows. At present, the main type of implants used in dental implantology are intraosseous osseointegratable implants, which require the presence of a sufficient volume of bone in the areas of implantation. The success of treatment with dental implants depends not only on the amount of available bone in the area designated for implantation, but also on its quality.

In daily practice, it is not uncommon to observe cases of deteriorated conditions for implant rehabilitation, such as bone with insufficient density type D4, characterized by fine spongiosis and lack of compact, as well as a reduced volume of available bone in the edentulous areas in horizontal and vertical direction. The causes of bone deficiency can be divided into two main groups – of pre-extraction and post-extraction period.

The first group of causes preceding the extraction contains two subgroups - anatomical variations, such as dehiscences, fenestrations and pneumatic sinus type on the one hand, and pathological processes on the other. The unfavorable reasons so described in this way are a frequent clinical picture in the distal sections of the upper jaw, where one of the anatomically important objects for implantation is located - the maxillary sinus. It belongs to the group of paranasal sinuses. The alveolar bone in the distal part of the upper jaw appears below the maxillary sinus, called the subantral bone. Part of the reasons for the bone deficiency in this area may be anatomical. In one group of patients, the maxillary sinus is relatively small and narrow with sufficient volume of alveolar bone - sclerotic type, while in others the

cavity is widely exposed and a reduced volume of subantral bone - pneumatic type, is observed. Sometimes, in the pneumatic type of maxillary sinus, the alveolar bone is so reduced in volume that the apexes of the upper maxillary molars protrude into the cavity.

The second group of causes for bone deficiency appears in the post-extraction period – the resorption of the alveolar bone itself and the afunctional atrophy caused by the lack of load on the alveolar bone for a long period of time.

Modern dental implantology has a number of methods for solving problems related to bone deficiency, which are summarized in three main groups. The first group of methods includes measures to prevent or minimize the bone deficiency in the post-extraction areas. The second group aims to increase the available bone volume and includes a number of methods of bone augmentation - guided bone regeneration, split - osteotomy of the alveolar ridge, block - grafting and elevation the maxillary sinus floor. The third group of methods are alternatives to intraosseous implants combined with bone augmentation.

The problems arising from the presence of bone deficiency in the areas for implant placement, such as the impossibility of placement in a prosthetically correctly planned position, along with the achievement of the mandatory high level of aesthetics in a large number of cases, as well as the prevention of biological and technical complications, necessitate the bone augmentation, as the most commonly used method to increase the available bone volume. Immediately after the guided bone regeneration, there comes the method of elevation the floor of the maxillary sinus as an augmentation procedure to increase the available volume of bone in the distal region of the upper jaw to achieve optimal rehabilitation with dental implants.

There exist a number of studies on the augmentation procedure for elevation the floor of the maxillary sinus with different techniques

and methods of execution. In most of them, the procedure is reported to be associated with a common, typical complication, perforation of the elevated sinus mucoperiosteum, as the perforation can be of various extent. In literature, there are various reports on the percentage prevalence of this complication - from 0 to 20.5%, and it has even been reported to reach 55%. This complication leads to compromising the graft and lowering the success rate of the subsequent implantological treatment.

Until now, the literature has not clarified the possibilities for optimizing the augmentation procedure for elevation the floor of the maxillary sinus with a lateral approach.

2. AIM AND TASKS

2.1. AIM OF THE THESIS

To explore the possibilities of optimizing the maxillary sinus floor elevation intervention.

To achieve this goal, the following tasks were set.

2.2. TASKS OF THE THESIS

2.2.1. To prepare a specification of available subantral bone in cases with maxillary sinus floor elevation.

2.2.2. To analyze the methods for the application of implants in conditions of subantral deficiency compared to the available subantral bone in cases with a maxillary sinus floor elevation.

2.2.3. To explore the possibilities of endoscopic approach.

2.2.4. To analyze clinical observations on approach for endoscopic control in maxillary sinus floor elevation.

3. INDIVIDUAL RESEARCH

3.1. MATERIALS AND METHODS

3.1.1. Materials and methods for task 1.

For the implementation of task №1 we performed a monocentric, retrospective study of preoperative CBCT images, taken at the X-ray Diagnostic Department of the University Medical and Dental Center of Medical University – Varna, Bulgaria on patients, who underwent maxillary sinus floor augmentation procedure with lateral approach (MSFALA), unilateral or bilateral, with the simultaneous or delayed dental implants placement for rehabilitation of the masticatory apparatus in the period 2014 to 2021.

The study included 76 3D images of the entire maxilla and MS in which no alteration in the sinus mucoperiosteum was observed, i.e., Schneiderian membrane thickness < 2 mm. Selected images ranged from single edentulous sections in the region of the first maxillary molar, partially distally restricted and unrestricted edentulous sections to totally edentulous maxilla. Since the study conducted was retrospective, indications for CBCT imaging could not be defined. Patients included in the study signed an informed consent stating that the imaging data obtained may be used for research.

The apparatus that was used for the study was "Planmeca ProMax 3D Max", integrated with a computer configuration "Hewlett-Packard" with a hard disk and peripherals for archiving information, image processing software "Planmeca Romexis" and a patient registration software. The time for which the device performs a scan is 9-40s, and the reconstruction of the image takes place in 2-55s. CBCT image saving and reading is carried out by means of "Planmeca Romexis" software, working with operating systems "Windows XP; Vista; 7; 8; 8.1 and 10 " of Microsoft.

The field of interest (FOV) when scanning can vary from a minimum of 50x55mm for sector image and maximum 230x260 mm for whole skull scanning. When scanning to obtain an image of the

jaws and maxillary sinus, the FOV varies between 130x90 mm and 130x160 mm.

Voxels are isotropic, in other words absolutely symmetrical in all three dimensions (directions) (X, Y, Z). Their sizes vary between 75µm for sector images up to 600 µm when scanning jaws and whole skull. The smaller the voxel size, the higher the resulting resolution and the greater the amount of data that can be obtained from the scanned image.

The arm of the device can be rotated from 210º to 360º. Radiation doses are measured in microSieverts and vary depending on the volume of the image.

At small image volume - 19 to 652 microSieverts, at medium volume – 45 to 860 microSieverts, and at large image volume – 68 to 1073 microSieverts. For comparison, radiation doses for axial CT860 are 1500 microSieverts and for orthopantomography (OPG) are 9 to 24 microSieverts.

A total of 76 preoperative CBCTs of patients who underwent MSFA augmentation procedure with the lateral approach were reviewed. 50 of these patients were males (66%), and 26 were females (34%) (Figure 1)

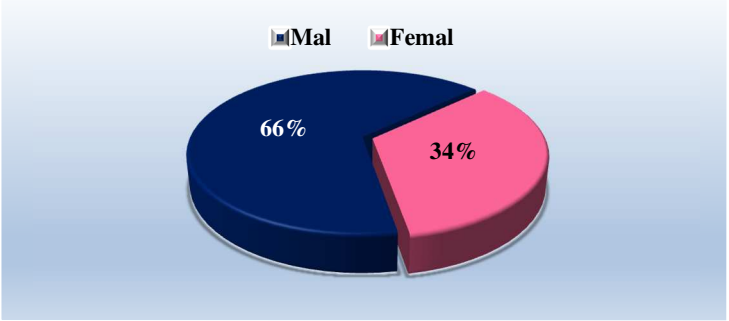

Figure 1. Graphical representation of the percentage distribution of patients by gender

The mean age of the male patients was 52,82 +/- 9,4 years (28-71). The mean age of the female patients was 47,19 +/- 10,6 years (25-68). Patients were divided according to the World Health Organization (WHO) age group classification (Aging classify cation according to WHO) (7). Patients whose preoperative CBCTs were included in the study were arranged in the following age groups according to the WHO age group classification: 15-44 years (young age) were 21 patients (27%), 45-59 years (middle age) were 40 patients (53%) and 60-74 years (elderly) were 15 patients (20%). In the young age group, there were 21 patients in total; 9 of them were male and represented 18% of the total number of males, and 12 were female and represented 46.2% of the total number of females. There were 40 patients in the middle-aged group, 29 of whom were male and accounted for 58% of the total number of males, and 11 of whom were female and accounted for 42.3% of the total number of females. In the elderly group, there were 15 patients; 12 of them were male, accounting for 24% of the total number of males, while females were three and accounted for 11.5% of the total number. Groups 0-14 years (childhood), 75-89 years (old age) and 90 + years (longevity), did not include any patients in the study (Figure 2).

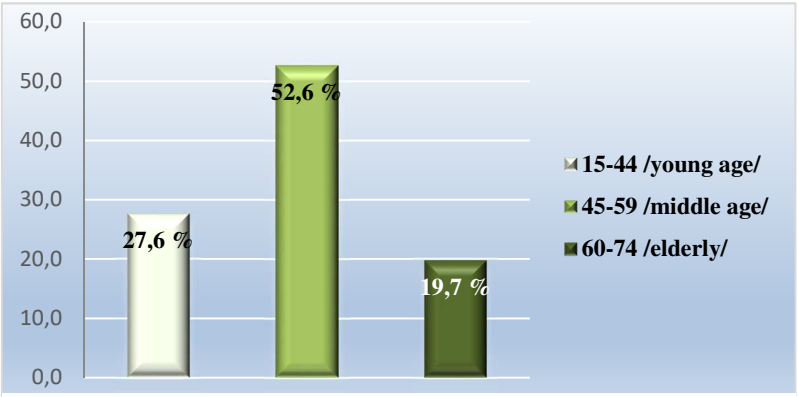

Figure 2. Graphical representation of the percentage distribution of patients by age group

Of the 76 preoperative CBCTs of patients who underwent MSFA with lateral approach, 108 maxillary sinuses were observed, and a total of 305 missing teeth were found.

These 305 missing teeth were divided according to the size of the defect and the number of missing teeth in it according to the FDI into six groups. In all 108 sinuses observed, the first molar was missing (whether 16 or 26 is meant denoted as region M_1). The first group includes 8 of the observed sinuses. The absence of the first molar is independent, representing 7% of the observed sinuses and 3% of all missing teeth.

The second group represents a defect of two missing teeth, the second premolar and the first molar (whether we consider 15 and 16 or 25 and 26, we designate them as region PM_2 and M_1). This defect was observed in 7 of all 108 sinuses, representing 7% of these and 4% of all missing teeth.

Third group, missing first and second molars (whether 16 and 17 or 26 and 27 we denote as region M_1 and M_2), with the number of this type of defect observed in 31 of all 108 sinuses observed. This represents 29% of the observed sinuses and 20% of the total number of missing teeth.

A fourth group, missing first and second premolars and first molars (whether 14, 15, and 16 or 24, 25, and 26, we designate as region PM_1, PM_2 and M_1), with the number of this type of defect observed in 4 of all 108 sinuses observed. This represents 4% of the observed sinuses and 4% of the total number of missing teeth.

The fifth group, missing second premolars, first and second molars (whether 15, 16, and 17 or 25, 26, and 27, we designate as region PM_2, M_1 and M_2), with the number of this type of defect observed in 23 of all 108 sinuses observed. This represents 21% of the observed sinuses and 23% of the total number of missing teeth. The sixth group, missing first and second premolars, first and second molars (whether 14, 15, 16, and 17 or 24, 25, 26, and 27, we designate

as region PM_1, PM_2, M_1 and M_2), with the number of this type of defect observed in 35 of all 108 sinuses observed. This represents 32% of the observed sinuses and 46% of the total number of missing teeth. (Figure 3 and 4).

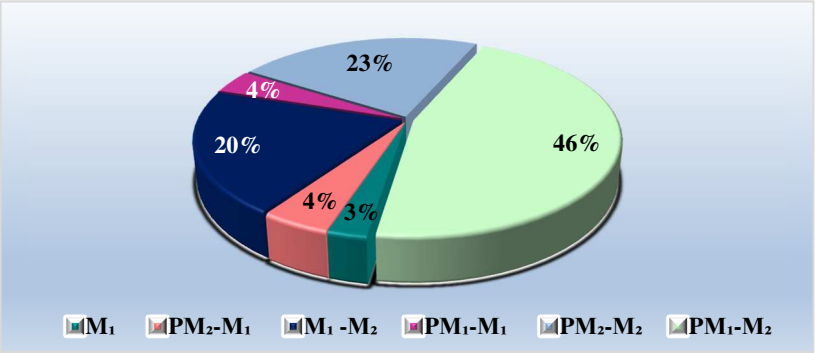

Figure 3. Graphical representation of the percentage distribution of the size of the edentulous defect and the number of missing teeth in it compared to the total number of missing teeth

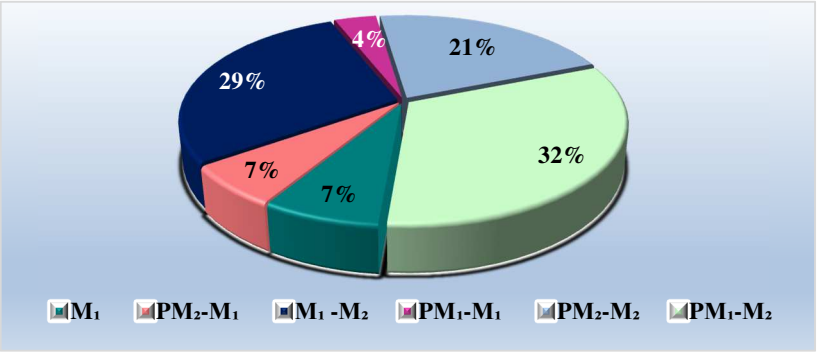

Figure 4. Graphical representation of the percentage distribution of the size of the edentulous defect and the number of missing teeth in it relative to the total number of observed sinuses

In all 76 preoperative CBCT studies of patients and all 108 observed sinuses, each of the 305 missing teeth observed on the paraxial section of the CBCT was measured the following three criteria, measured in milimeters:

- subantral bone height (SBH) in the region of the missing tooth, starting from the ridge of the alveolar ridge to the floor of the maxillary sinus (Figure 5).
- subantral bone width (SBW) in the missing tooth region, taking as a starting point the distance between the vestibular and palatal compacts of the alveolar ridge in the vestibule-palatal direction (Figure 6).
- maxillary sinus width (MSW), starting from the medial and lateral walls of the maxillary sinus in the vestibular-palatal direction at a distance of 8 mm from the ridge of the alveolar ridge, and this parameter is measured only in regions of missing teeth, where SBH < 8 mm. (Figure 7)

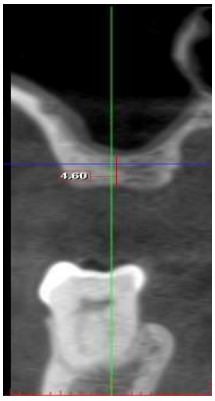

Figure 5. subantral bone height(SBH)

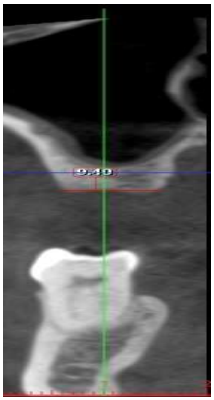

Figure 6. subantral bone width(SBW)

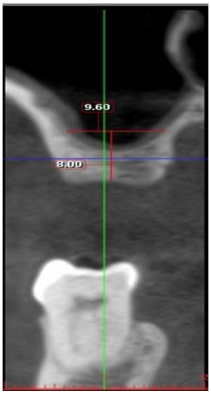

Figure 7. maxillary sinus width(MSW)

3.1.2. Materials and methods for task 2.

For the implementation of task №1 we performed a monocentric, retrospective study of preoperative CBCT images, taken at the X-ray Diagnostic Department of the University Medical and Dental Center of Medical University – Varna, Bulgaria on patients, who underwent maxillary sinus floor augmentation procedure with lateral approach (MSFALA), unilateral or bilateral, with the simultaneous or delayed dental implants placement for rehabilitation of the masticatory apparatus in the period 2014 to 2021 by four operators - doctors of dental medicine. The study included 76 three-dimensional images of the entire upper jaw and maxillary sinuses, in which no change was observed in the sinus mucoperiosteum, i.e. the thickness of Schneider's membrane $\leq$ 2 mm. The selected images range from single edentulous areas in the maxillary first molar region, partially distally limited and unlimited edentulous areas to a totally edentulous maxilla. Since the study was retrospective, indications for CBCT imaging cannot be defined. The patients included in the study have signed an informed consent that the data from the obtained images, as well as the information about their implant-prosthetic treatment, can be used for scientific research.

The apparatus that was used for the study was "Planmeca ProMax 3D Max", integrated with a computer configuration "Hewlett-Packard" with a hard disk and peripherals for archiving information, image processing software "Planmeca Romexis" and a patient registration software. The time for which the device performs a scan is 9-40s, and the reconstruction of the image takes place in 2-55s. CBCT image saving and reading is carried out by means of "Planmeca Romexis" software, working with operating systems "Windows XP; Vista; 7; 8; 8.1 and 10 " of Microsoft.

The field of interest (FOV) when scanning can vary from a minimum of 50x55mm for sector image and maximum 230x260 mm

for whole skull scanning. When scanning to obtain an image of the jaws and maxillary sinus, the FOV varies between 130x90 mm and 130x160 mm.

Voxels are isotropic, in other words absolutely symmetrical in all three dimensions (directions) (X, Y, Z). Their sizes vary between 75µm for sector images up to 600 µm when scanning jaws and whole skull. The smaller the voxel size, the higher the resulting resolution and the greater the amount of data that can be obtained from the scanned image.

The arm of the device can be rotated from 210º to 360º. Radiation doses are measured in microSieverts and vary depending on the volume of the image.

At small image volume - 19 to 652 microSieverts, at medium volume – 45 to 860 microSieverts, and at large image volume – 68 to 1073 microSieverts. For comparison, radiation doses for axial CT860 are 1500 microSieverts and for orthopantomography (OPG) are 9 to 24 microSieverts.

Forty-four patients (57.9%) whose preoperative CBCTs were included in the study had a unilateral MSFALA, and 32 patients (42.1%) had a bilateral MSFALA.

Out of a total of 76 preoperative CBCTs of patients examined, a MSFALA augmentation procedure was performed on 108 maxillary sinuses, and a total of 305 missing teeth were identified. The absence of these teeth was rehabilitated with 161 implants according to data from the patients' medical records. The application of implants in conditions of subantral deficiency by the four operators was carried out using two methods - maxillary sinus floor augmentation procedure with lateral approach with immediate implant placement (MSFALAIIP) and maxillary sinus floor augmentation procedure with lateral approach with delayed implant placement (MSFALADIP).

In 70 cases of MSFALA, a MSFALAIIP method was used for the application of implants in conditions of subantral deficiency (65%), and in 38 cases MSFALADIP was used (35%) (Figure 8).

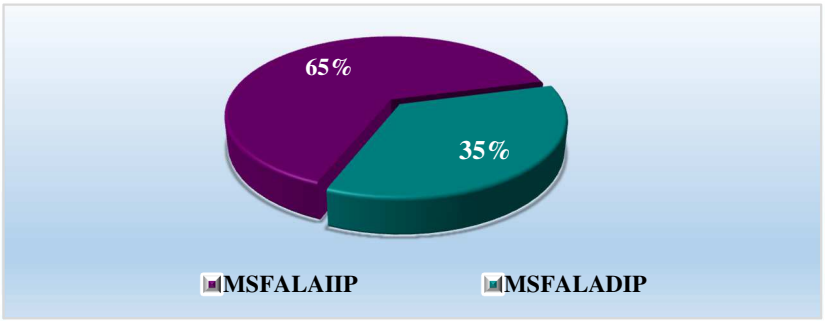

Figure 8. Graphical representation of the percentage distribution of a method for the application of implants in conditions of subantral deficiency

The method for the application of implants in conditions of subantral deficiency MSFALAIIP was used by operator 1 in 27 (39%) maxillary sinuses, by operator 2 in 21 (30%), by operator 3 in 15 (21%) and by operator 4 in 7 (10%) (Figure 9).

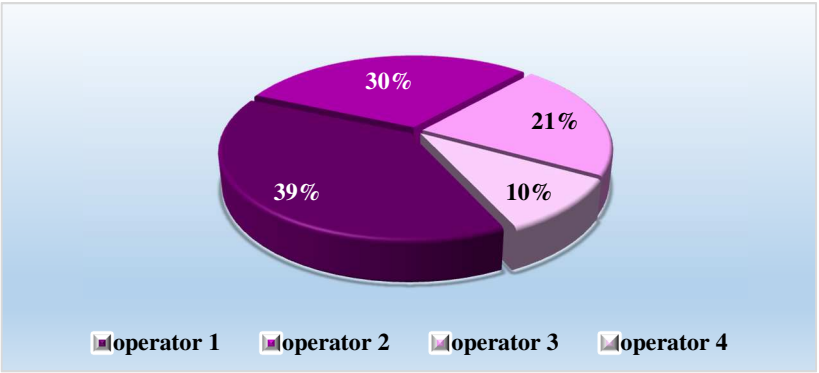

Figure 9. Graphical representation of the percentage distribution of a method for the application of implants in conditions of subantral deficiency MSFALAIIP by operators

The method for the application of implants in conditions of subantral deficiency MSFALADIP was used by operator 2 in 19 (50%) maxillary sinuses, by operator 3 in 14 (37%) and by operator 4 in 5 (13%). Operator 1 did not apply the method for the application of implants in conditions of subantral deficiency MSFALADIP in his/her clinical cases (Figure 10)

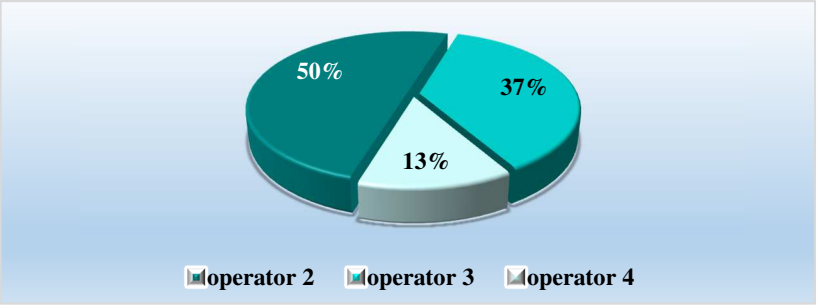

Figure 10. Graphical representation of the percentage distribution of a method for the application of implants in conditions of subantral deficiency MSFALADIP by operators

Of the one hundred and sixty-one implants placed, the application of 100 (62%) of them was using the MSFALAIIP method, and 61 (38%) with the MSFALADIP method (Figure 11)

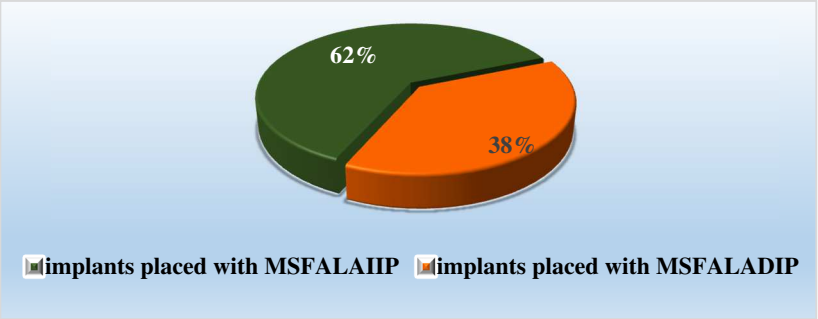

Figure 11. Graphical representation of the percentage distribution of a method for the application of implants in conditions of subantral deficiency MSFALAIIP by method

The distribution of the hundred implants with the MSFALAIIP method by operators is as follows - by operator 1 there are 38 (38%), by operator 2 - 28 (30%), by operator 3 - 22 (22%) and by operator 4 - 12 (12%) (Figure 12).

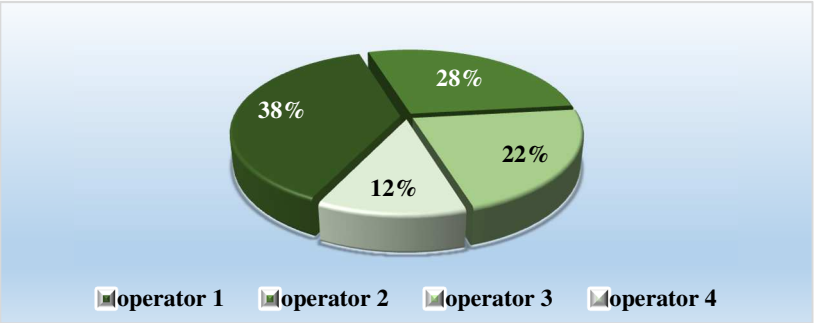

Figure 12. Graphical representation of the percentage distribution of a method for the application of implants with MSFALAIIP by operators

The allocation of implants using the MSFALADIP method by operator 2 in 30 (49%), by operator 3 in 24 (39%) and by operator 4 in 7 (12%). There is no data on implant application using the MSFALADIP method for operator 1 (Figure 13).

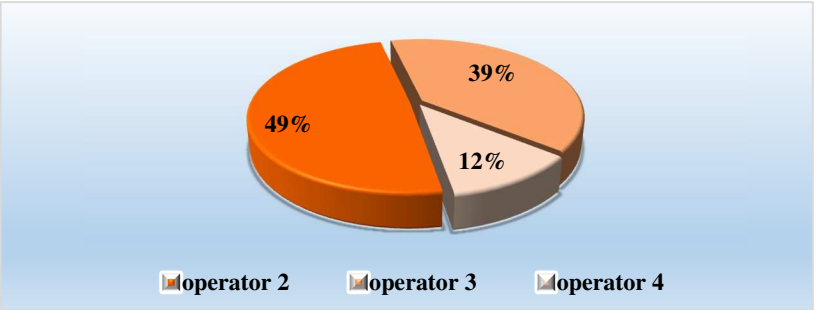

Figure 13. Graphical representation of the percentage distribution of a method for the application of implants with MSFALADIP by operators

In all 76 examined preoperative CBCT examinations of patients and all 108 observed sinuses, a measurement of the SBH was made in each of the 161 areas with performed MSFALAIIP and/or MSFALADIP. The measurement was made on a paraxial section of the preoperative cone-beam tomography, taking the distance from the crest of the alveolar ridge to the floor of the maxillary sinus as reference points (Figure 14).

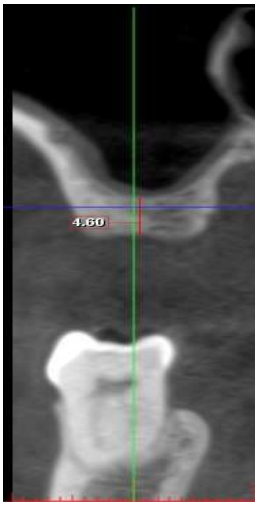

Figure 14. subantral bone height (SBH)

The data on the SBH were analyzed according to a method for the application of implants in conditions of subantral deficiency MSFALAIIP and MSFALADIP with the help of IBM SPSS Statistics 25. To prepare the statistical analysis of the collected data, the following statistical methods were applied - non-parametric tests - Mann-Whitney test (U - test) for two independent samples and Kruskal-Wallis test for comparing more than two groups.

3.1.3. Materials and methods for task 3.

For the implementation of task №3 we performed an experimental study was conducted on maxilla and maxillary sinuses three-dimensional simulation models. For the development of these three-dimensional simulation models, 20 preoperative CBCT images taken at the X-ray Diagnostic Department of the University Medical and Dental Center of Medical University – Varna, Bulgaria of patients who underwent MSFALA unilateral or bilateral, with the simultaneous or delayed dental implants placement for rehabilitation of the masticatory apparatus in the period 2014 to 2021 were selected.

To perform the study, we selected 20 preoperative CBCT images of patients who underwent bilateral sinus floor elevation with

a lateral approach and measured the height of the available subantral bone in the areas submitted to the augmentation maxillary sinus floor elevation procedure between 2 - 4 mm. The preoperative CBCT images selected to produce the 3D models were of 10 male and 10 female patients.

Using the CBCT image processing software "Planmeca Romexis", an image is generated from which an STL file is output. The "Planmeca Romexis" software allows to produce a higher quality STL file by selecting the resolution and the visualization of the object to be exported, also selecting the directory to export and naming the file. We visualize the generated STL files using the software program "Autodesk Meshmixer", in order to further process the image - cleaning from artifacts. When processing the images in the program they automatically acquire *mix. extension. The prepared images that we want to print need to be displayed again in STL format.

The prepared STL files of the 3D models were printed using the "Visions3Dprinter" of the manufacturer 3Dfactories. The working principle of this printer is FDM (Fused Deposition Modeling) - the model is built by applying a melted material (PLA - filament) through an extruder (nozzle) heated to 200º, which is part of an extrusion head that moves horizontally (“X” and “Y” axis), layer by layer along a defined path on a movable in the vertical direction (“Z” axis to 150 mm) table with dimensions 150 x 150 mm. The material the printer works with is a thermoplastic polymer - polylactic acid (PLA). The material is a filament with a diameter of 1,75 mm wrapped on a roll. The extruder of the printer has a diameter of 0,3 mm, the maximum printing speed is 80 mm/s, there is a built-in LED lighting that allows the printing process to be monitored. The printer works with a software program to prepare for printing models - "3Dfactories - Repetier - Host V1.0.6" (Figure 15).

Figure 15. "Visions3Dprinter" на 3Dfactories.

The ready STL files are prepared for printing using "3Dfactories - Repetier - Host V1.0.6", and for all 20 models the same individual printing parameters are set to meet the needs of our task - model build quality - 0.08 mm (High quality), type of adhesion of the model to the table - Raft and model maintenance by touching the table. The printing speed and the printing speed of the outer perimeter of the printed model is the same - 38mm/s - slow type. Fill speed is 45mm/s and density is 60%. After setting the parameters in this way, the STL files are subjected to slicing with CuraEngine. After the slicing is completed, the software program visualizes the future 3D simulation model by predicting the printing time, the total number of layers, the total number of rows to be applied layer by layer and the required amount of filament in mm.

Before printing the 3D stimulation model we set the individual print values of the 3D printer, which are: print speed and filament feed speed (filament) - 100, running cooling function - fan and extruder heating to 200 º. After the extruder reaches the temperature of 200 º, the printing is started.

During printing of the 3D simulation models, there is a visualization of the extruder head itself moving in the layer application order preset by CuraEngine. This allows the printing to be monitored and, if an error occurs, stopped for debugging.

Once the 3D simulation models have completed the printing process, they are carefully detached from the printer table. The models are subjected to cleaning from the support elements. The 3D simulation models are scaled 1:1 relative to the patients (Figure16).

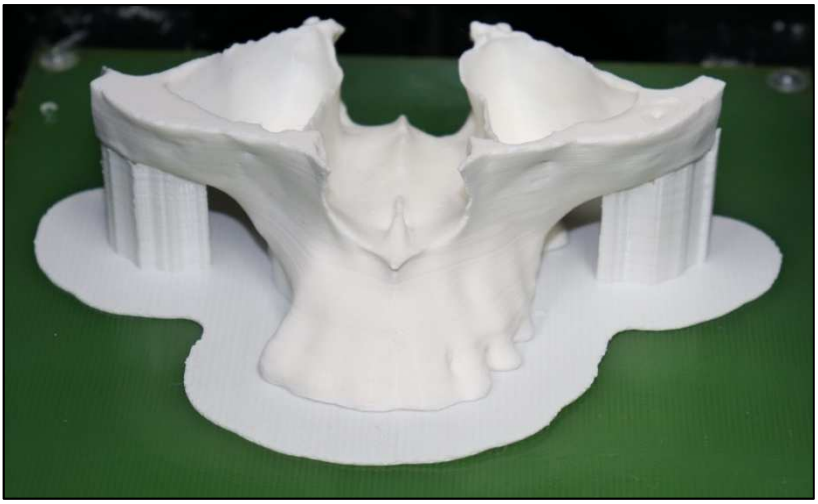

Figure 16. The 3D simulation models

On each sinus of the 3D models, a visibility fraction measurement of the maxillary sinus total surface area in the antero-posterior direction was conducted using a Karl Storz ENDOCAMELEON ENT HOPKINS Telescope with built-in optics with the angled visual axis deflected from 15º - 90º to the instrument axis (Figure 17).

Figure 17. ENDOCAMELEON ENT HOPKINS Telescope Karl Storz

In order to conduct the study of each 3D model in the antero-posterior direction, a millimetre paper was placed on each maxillary sinus floor, whose length was individualized according to the individual characteristics of each patient and its width is 5 mm (Figure 18).

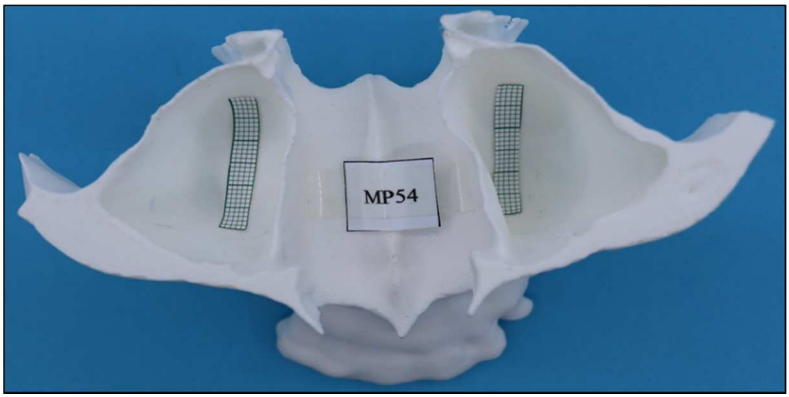

Figure 18. A printed 3D model with placed millimetre paper on the sinus floor

Measurement of share of visibility (SV) of the maxillary sinus total surface area was performed with the visual axis deflected to 15º, 45º and 90º to the instrument axis. SV of the maxillary sinus total surface area is established by relating the individual maxillary sinus length to the observed instantaneous length at the different visual axes of the selected 15º, 45º and 90º. (Figure 19, 20, 21).

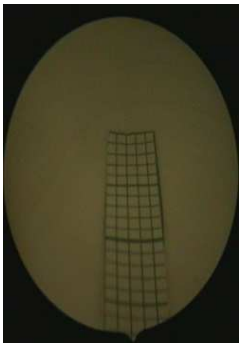

Figure 19. SV with the visual axis deflected to 15⁰ to the instrument axis

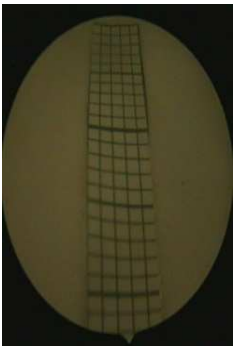

Figure 20. SV with the visual axis deflected to 45⁰ to the instrument axis

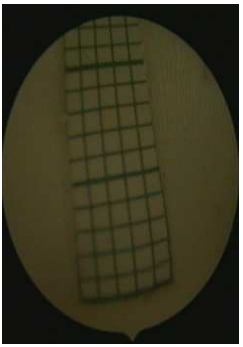

Figure 21. SV with the visual axis deflected to 90⁰ to the instrument axis

SV is measured on 40 maxillary sinuses of 20 3D simulation models. The endoscopic access through which the measurement is performed using a trocar-guided endoscopic technique, which requires a trocar with an outer diameter of 5 mm and a cannula with a fenestrated tip of 5 mm in diameter and 85 mm in length (Figure 21)

Figure 21. A trocar with an outer diameter of 5mm and a cannula with a fenestrated tip with a diameter of 5mm

On each maxillary sinus anterior wall, three openings, medial, central and distal, were performed by using a 5 mm diameter trocar with a distance of 8 mm between the centres of the holes. To locate the centre of the medial opening, the projection of the canine tooth 5 mm in vertical direction and then 5 mm in distal direction is taken as starting point (Figure 22 and 23)

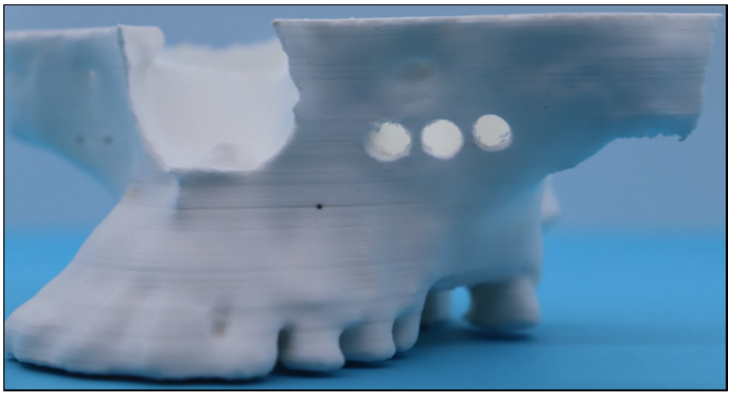

Figure 22. A printed 3D model with three holes created – medial central and distal

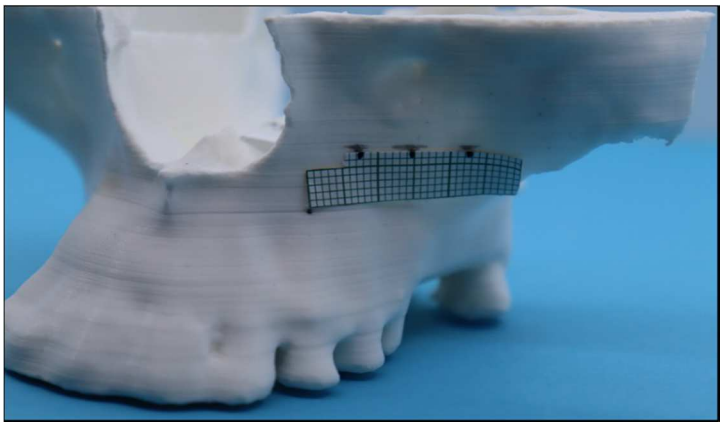

Figure 23. A printed 3D model on which the positions of the centers of the holes to be created are marked.

To measure SV of the MSF total area, the endoscope was advanced in the antero-posterior direction 10 mm and 20 mm into each performed medial, central and distal opening of each sinus, which was observed at visual axes 15º, 45º and 90º to the instrument axis and the lowest focal angle.

SV data of the maxillary sinus total surface area was analyzed against the endoscopic access opening, endoscope penetration depth, and endoscope viewing angle using IBM SPSS Statistics 25. The following statistical methods were applied to perform the statistical analysis of the collected data: parametric tests - Student's t-test for dependent samples and ANOVA - test to compare more than two groups and non-parametric tests - Wilcoxon test for dependent samples, Kruskal -Wallis and Fridman test to compare more than two groups.

3.1.4. Materials and methods for task 4.

For the implementation of task № 4, a prospective clinical study was conducted at the University Medical Dental Center (UMDC) whose object were ambulatory patients with observed deteriorated conditions for rehabilitation by implant treatment. The twenty-three patients included in the study underwent a planned unilateral surgical intervention through an endoscopically navigated augmentation procedure for MSFALA

The aim of the present study is to evaluate the approach for endoscopic control in the augmentation procedure by MSFALA.

The study was approved by decision of the Research Ethics Committee (REC) No. 116/28.04.2022 at Medical University - Varna "Prof. Dr. Paraskev Stoyanov".

Criteria for inclusion in the study:

- Persons aged 18 to 74 years.
- Patients with single edentulous areas in the upper first molar area, partially distally limited and unlimited edentulous areas up to totally edentulous upper jaw.
- Patients with established presence of subantral bone height on preoperative CBCT ≤ 6 mm.
- Patients with no changes observed in the sinus mucoperiosteum.
- A completed and signed informed consent form.

Criteria for exclusion from the study:

- Persons under 18 years of age.
- Patients with established presence of subantral bone height on preoperative CBCT ≥ 6 mm.
- Patients with observed changes in the sinus mucoperiosteum, with a thickening of Schneider's membrane ≥ 2mm.
- Persons who do not have a completed and signed declaration of informed consent.

4.4.1. Preoperative preparation.

All patients underwent a preliminary primary consultation for implant treatment, in order to assess the functional state of the masticatory apparatus, and a preoperative CBCT was assigned, to assess the SBH, the anatomical variations of the MS were analyzed (the presence of full/ and/or partial septa, prominent tooth roots, the thickness of the Schneider's membrane) and the planning of the osteotomy to create an approach window at the site of the planned augmentation. Patients filled out and signed a Questionnaire on

General Health, Declaration of Informed Consent for X-ray Examination.

The patients underwent a preliminary anesthesia consultation before the operation by an anesthesiologist-resuscitator according to the rules and protocols adopted in the operating block of the UMDC, during which they filled in and signed a Preoperative Anesthesia Consultation and Assessment Sheet and a Protocol for a preliminary explanatory conversation about anesthesia between the patient and the anesthetist. Before performing an endoscopically navigated MSFALA, patients fill out and sign a Declaration of Informed Consent regarding the implementation of medical-dental diagnostic and treatment activities at the University Medical-Dental Center.

4.4.2. Treatment methods.

For all patients, the endoscopically navigated MSFALA was performed in the conditions of an operating block located in the UMDC - Varna, and all measures for asepsis and antiseptics were observed. In all cases, for the purposes of the surgical intervention, general, intubation anesthesia was used, performed by an anesthesiologist - resuscitator according to the rules and protocols adopted in the operating block of the UMDC. All twenty-three endoscopically navigated MSFALA were performed by a single operator, with the endoscopic approach opening making was timed using a stopwatch in seconds. Also, according to a modified subjective scale PFS-12 (Piper Fatigue Scale - 12), the fatigue of the operator was recorded immediately after making the opening (12) (Table 1).

The subjective assessment of fatigue /digital/	Interpretation of the numerical scale
0	Lack of fatigue
1-3	Mild fatigue
4-6	Moderate intensity fatigue
7-9	Severe fatigue
10	The strongest possible fatigue

Table 1. The subjective assessment of fatigue by operator

4.4.2.1. Method of approach for endoscopic control during an MSFALA.

In all patients, the endoscopically navigated MSFALA was performed using an ENDOCAMELEON ENT HOPKINS Telescope Karl Storz endoscope with built-in optics with an angled visual axis deviated from 15º - 90º to the axis of the instrument. The observation was carried out with a visual axis deviated at 45º to the axis of the instrument and the lowest focal angle when entering it in the antero-posterior direction at 10 mm. In all patients, before using the endoscope, it is necessary that its camera underwent preliminary preparation in order to eliminate the formation of condensation on it, consisting in wiping the camera with sterile gauze soaked in sterile sodium chloride solution at room temperature. Endoscopic approach was performed through the fossa canina.

We divided the patients included in the study into two groups according to the technique used in making the opening providing the endoscopic approach through the fossa canina. Two techniques were used – trocar guided and machine osteotomy.

Group I – included twelve patients in whom the opening providing endoscopic approach was made by machine osteotomy using a calibrated osteotome drill with a diameter of 4.2 mm. All patients in the area of the planned fossa canina approach were administered local anesthesia using a 4% solution of articaine with adrenaline 1/100,000 (Septanest). To find the center of the fossa canina approach hole, one took the canine apex projection 5 mm vertically and then 5 mm distally as a starting point. Due to the diameter of the osteotome drill with which the opening was created, it was necessary to measure another 2 mm in the vertical direction and 2 mm in the distal direction. A 10 mm incision was made with soft tissue dissection, the osteotomy for endoscopic approach was performed using an implantology unit (iChiropro 1600784-001, Bien Air Dental, Switzerland) with a 20:1 reduction tip and a calibrated osteotome drill with a diameter of 4,2 mm (Figure 24 and 25), at a rotation speed of 1,000 rpm. and continuous cooling with 0.9% sterile sodium chloride solution.

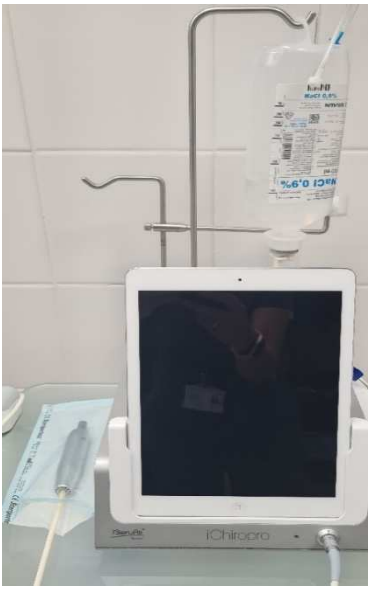

Figure 24. Implantology unit (iChiropro 1600784-001, Bien Air Dental, Switzerland)

The use of the endoscope for observation was accomplished by means of a STAMMBERGER telescopic round cannula 14,5 sm long and 4 mm in diameter (Figure 26).

Figure 25. Calibrated osteotome drill with a diameter of 4,2 mm

Figure 26. ENDOCAMELEON ENT HOPKINS Telescope Karl Storz and telescopic round cannula STAMMBERGER with long 14,5 sm and 4 mm in diameter

Group II - included eleven patients in whom the opening providing endoscopic approach was made by a trocar-guided technique using a trocar with an outer diameter of 5 mm and a cannula with a fenestrated tip 5 mm in diameter and 85 mm long. The fenestrated tip of the cannula served for endoscope lens bed (Figure 27). All patients in the area of the planned fossa canina approach were administered local anesthesia using a 4% solution of articaine with adrenaline 1/100,000 (Septanest). To find the center of the fossa canina approach hole, one took the canine apex projection 5 mm vertically and then 5 mm distally as a starting point. Due to the diameter of the trocar used to create the opening, it was necessary to measure another 2.5 mm in the vertical direction and 2.5 mm in the distal direction. By means of operator's pressure on the trocar, the soft tissues and the front wall of the MS were fenestrated, and the opening

was formed by the compression that the operator exerted on the trocar and the rotary-progressive movements for additional shaping.

Figure 27. ENDOCAMELEON ENT HOPKINS Telescope Karl Storz, cannula with a fenestrated tip 5 mm in diameter and 85 mm long and trocar with an outer diameter of 5 mm

4.4.2.2. Method of MSFALA

All patients underwent local anesthesia in the area of planned approach to the lateral wall of the maxillary sinus using a 4% solution of articaine with adrenaline 1/100,000 (Septanest). *MSFALA* was performed after dissection of a mucoperiosteal flap providing approach to the lateral wall of the MS. The osteotomy to create an approach window was performed using an implantology unit, a straight surgical handpiece, and a 4 mm diameter round head diamond surgical bur at a rotation speed of 30,000 rpm. and continuous cooling with 0.9% sterile sodium chloride solution. After the osteotomy was completed, one proceeded to dissection of the sinus mucoperiosteum with the help of sinus elevators in a vertical direction, which formed a cavity with a planned height. One proceeded to implant osteotomy in the SBH, during which there was protection of the already elevated sinus mucoperiosteum with the help of a sinus elevator. After

finalizing the implant osteotomy, a collagen fleece (Collagen fleece Botiss, Berlin, Germany) was placed on the ceiling of the grafting cavity, the implants were placed in the implant osteotomy in order to avoid collapse of the elevated sinus mucoperiosteum with the collagen fleece, then there followed the application of the bone restoration material - nanohydroxylapatite aqueous gel with two-phase calcium phosphate ceramic particles (Maxresorb Inject Botiss, Berlin, Germany). The approach window was covered with a pericardial collagen barrier membrane (Jason Membrane Botiss, Berlin, Germany) that covers at least 2 mm of the bone edge of the approach window. The flap was repositioned, adapted and sutured using 5/0 monofilament suture (Dafilon, BBraun, Germany).

After performing the endoscopically navigated *MSFALA*, patients undergo a stay in a day hospital with observation for up to 12 hours. All patients were administered antibiotic protection for 5 to 7 days to prevent postoperative infection.

3.2. RESULTS

3.2.1. Results for task 1.

The obtained data for the three criteria SBH, SBW, and MSW for regions PM_1, PM_2, M_1 и M_2 set out in Table 2.

	Researched criteria, mm	n area	Mean	SD	Median	Q_1	Q_3	IQR	Range	Min	Max
region PM_1	SBH	39	10,80	3,31	x	x	x	x	12,90	4,31	17,21
	SBW	39	6,27	2,07	x	x	x	x	7,34	2,33	9,67
	MSW	8	5,98	2,31	x	x	x	x	6,00	3,40	9,40
region PM_2	SBH	69	x	x	6,12	4,50	7,61	3,11	16,93	1,61	18,54
	SBW	69	6,28	2,02	x	x	x	x	9,81	1,80	11,61
	MSW	55	x	x	7,21	5,40	8,20	2,80	11,17	2,83	14,00
region M_1	SBH	108	x	x	3,20	2,20	4,60	2,40	5,80	1,00	6,80
	SBW	108	x	x	6,80	5,30	8,20	2,90	11,40	2,60	14,00
	MSW	108	x	x	10,60	9,26	12,75	3,49	13,40	5,80	19,20
region M_2	SBH	89	3,62	1,72	x	x	x	x	6,60	1,00	7,60
	SBW	89	8,50	2,78	x	x	x	x	12,00	3,00	15,00
	MSW	89	11,40	2,95	x	x	x	x	12,80	6,00	18,80

Table 2. The obtained data for the three criteria SBH, SBW and MSW for regions PM_1, PM_2, M_1 и M_2

3.2.1.1. Analysis by patient's gender.

The obtained and analyzed data for the three criteria SBH, SBW and MSW in relation to the patient's gender are shown in table 3

	Researched criteria, mm	n area	sex	Mean	SD	Median	Q_1	Q_3	IQR	Range	Min	Max	t	U test	P
region PM_1	SBH	24	*male*	11,42	3,39	x	x	x	x	12,37	4,84	11,21	1,54	x	0,133
		15	*female*	9,81	3,02	x	x	x	x	11,29	4,31	15,60			
	SBW	24	*male*	6,83	2,08	x	x	x	x	7,26	2,41	9,67	2,31	x	0,027
		15	*female*	5,38	1,79	x	x	x	x	5,76	2,33	8,00			
	MSW	5	*male*	6,68	2,19	x	x	x	x	5,40	4,00	9,40	x	x	x
		3	*female*	x	x	x	x	x	x	x	x	x			
region PM_2	SBH	46	*male*	x	x	6,31	5,16	8,00	2,84,	16,54	2,00	18,54	x	352,0	0,024
		23	*female*	x	x	5,97	3,21	6,40	3,19	6,71	1,61	8,32			
	SBW	46	*male*	6,68	1,99	x	x	x	x	9,76	1,85	11,61	2,46	x	0,017
		23	*female*	5,48	1,87	x	x	x	x	6,61	1,80	8,41			
	MSW	33	*male*	x	x	7,80	5,60	8,60	3,00	10,00	4,00	14,00	x	279,5	0,151
		22	*female*	6,73	2,07	7,00	5,25	7,61	2,36	8,97	2,83	11,80			
region M_1	SBH	71	*male*	3,54	1,43	3,40	2,40	4,60	2,20	5,25	1,00	6,25	x	1 176	0,373
		37	*female*	x	x	3,00	2,00	5,20	3,20	5,60	1,20	6,80			
	SBW	71	*male*	x	x	7,00	5,60	8,20	2,60	11,00	3,00	14,00	x	1 212	0,513
		37	*female*	6,73	2,51	6,55	4,50	8,40	3,90	9,01	2,60	11,61			
	MSW	71	*male*	x	x	10,40	9,00	12,60	3,60	13,39	5,81	19,20	x	1 465	0,327
		37	*female*	11,24	2,14	11,40	9,61	12,80	3,19	10,20	5,80	16,00			
region M_2	SBH	63	*male*	3,70	1,70	x	x	x	x	6,20	1,00	7,20	0,67	x	0,51
		26	*female*	3,43	1,79	x	x	x	x	6,60	1,00	7,60			
	SBW	63	*male*	9,02	2,64	x	x	x	x	11,19	3,81	15,00	2,79	x	0,01
		26	*female*	7,25	2,76	x	x	x	x	9,21	3,00	12,21			
	MSW	63	*male*	11,26	3,00	x	x	x	x	12,40	6,00	18,40	-0,70	x	0,49
		26	*female*	11,74	2,87	x	x	x	x	12,20	6,60	18,80			

Table 3. Data for the three criteria SBH, SBW and MSW in relation to the patient's gender

Region PM_1

The data analysis showed a statistically significant difference in the amount of SBW in the PM_1 region relative to the patient's gender $p<0,05$. There was no statistically significant difference in the size of SBH in the region of PM_1 relative to the gender of the patient $p>0,05$. Due to the small number of cases studied, no analysis of the size of MSW by gender was performed.

Region PM_2

Data analysis showed a statistically significant difference in the size of SBH and SBW in the PM_2 region relative to the patient's gender $p\leq0,05$. However, there was no statistically significant difference for MSW in PM_2 region relative to the patient's gender $p\geq0,05$.

Region M_1

The data analysis did not show a statistically significant difference in the size of SBH and SBW and MSW in the M_1 region according to the patient's gender $p\geq0,05$.

Region M_2

The data analysis revealed a statistically significant difference for SBW in M_2 compared to the gender of the patient $p\leq0,05$. However, there was no statistically significant difference in the size of SBH and MSW in the M_2 region relative to the patient's gender $p\geq0,05$.

3.2.1.2. Analysis by patient's age.

The obtained and analyzed data for the three criteria SBH, SBW and MSW in relation to the patient's age are shown in table 4.

	Researched criteria, mm	n area	Age grup	Mean	SD	Median	Q_1	Q_3	IQR	Range	Min	Max	ANOVA F	Kruskal Wallis	P
region PM_1	SBH	9	*15-44*	10,23	2,85	x	x	x	x	9,27	6,23	15,50	3,00	x	0,062
		18	*45-59*	9,86	3,52	x	x	x	x	12,33	4,31	16,64			
		12	*60-74*	12,64	2,72	x	x	x		9,05	8,16	17,21			
	SBW	9	*15-44*	5,33	1,94	x	x	x	x	5,59	2,41	8,00	6,67	x	0,003
		18	*45-59*	5,69	1,75	x	x	x	x	6,27	2,33	8,60			
		12	*60-74*	7,86	1,84	x	x	x	x	5,49	4,18	9,67			
	MSW	2	*15-44*	x	x	x	x	x	x	x	x	x	x	x	x
		6	*45-59*	5,51	2,28	x	x	x	x	6,00	3,40	9,40			
		x	*60-74*	x	x	x	x	x	x	x	x	x			
region PM_2	SBH	17	*15-44*	5,68	2,06	6,00	3,88	6,64	2,75	7,67	2,00	9,67	x	5,9	0.053
		35	*45-59*	5,68	2,17	5,97	4,20	6,75	2,55	8,99	1,61	10,60			
		17	*60-74*	x	x	7,44	5,36	8,00	2,64	14,94	3,60	18,54			
	SBW	17	*15-44*	5,42	1,96	x	x	x	x	7,15	1,85	9,00	2,6	x	0.082
		35	*45-59*	6,37	1,97	x	x	x	x	8,60	1,80	10,40			
		17	*60-74*	6,94	2,01	x	x	x	x	7,76	3,85	11,61			
	MSW	15	*15-44*	7,38	3,24	6,60	4,80	9,00	4,20	11,17	2,83	14,00	x	0,2	0.91
		30	*45-59*	7,35	2,18	7,60	5,70	8,26	2,56	10,18	3,42	13,60			
		10	*60-74*	x	x	7,20	5,85	7,80	1,95	7,58	5,22	12,80			
region M_1	SBH	31	*15-44*	3,60	1,43	3,20	2,40	4,40	2,00	5,60	1,20	6,80	x	1,77	0.412
		57	*45-59*	3,32	1,58	3,20	1,90	4,70	2,80	5,00	1,00	6,00			
		20	*60-74*	3,73	1,38	3,50	2,50	4,90	2,40	4,45	1,80	6,25			
	SBW	31	*15-44*	6,74	2,31	6,55	5,40	8,40	3,00	10,01	2,60	12,61	x	1,27	0.529
		57	*45-59*	6,95	2,55	6,80	5,20	8,20	3,00	9,80	3,00	12,80			
		20	*60-74*	x	x	7,20	5,67	9,90	4,23	10,00	4,00	14,00			
	MSW	31	*15-44*	10,94	2,39	10,46	9,20	12,60	3,40	10,20	5,80	16,00	x	1,36	0.506
		57	*45-59*	x	x	10,40	9,21	12,70	3,49	13,39	5,81	19,20			
		20	*60-74*	11,80	2,75	11,71	10,00	12,80	2,80	10,20	7,40	17,60			
region M_2	SBH	22	*15-44*	3,35	1,65	x	x	x	x	5,60	1,00	6,60	0.58	x	0.562
		49	*45-59*	3,63	1,82	x	x	x	x	6,60	1,00	7,60			
		18	*60-74*	3,94	1,54	x	x	x	x	5,40	1,40	6,80			
	SBW	22	*15-44*	8,03	2,62	x	x	x	x	9,00	3,00	12,00	0.83	x	0.439
		49	*45-59*	8,47	2,60	x	x	x	x	11,60	3,40	15,00			
		18	*60-74*	9,16	3,40	x	x	x	x	10,19	3,81	14,00			
	MSW	22	*15-44*	11,84	2,92	x	x	x	x	10,80	6,20	17,00	0.39	x	0.678
		49	*45-59*	11,17	3,09	x	x	x	x	12,40	6,00	18,40			
		18	*60-74*	11,50	2,72	x	x	x	x	10,60	8,20	18,80			

Table 4.Data for the three criteria SBH, SBW and MSW in relation to the patient's age

Region PM₁

The analysis of the data showed a statistically significant difference in SBW in the region of PM_1 compared to the patient's age $p \leq 0.05$. There was no statistically significant difference in SBH compared to the patient's age $p \geq 0.05$. Due to the small number of cases studied, no age-related analysis for MSW was performed.

Region PM₂

The data analysis showed a statistically significant difference in SBH in the PM_2 region compared to the patient's age $p \leq 0.05$. On the other hand, there was no statistically significant difference in SBW and MSW in the PM_2 region concerning the patient's age $p \geq 0.05$.

Region M₁

The data analysis did not show a statistically significant difference in SBH and SBW and MSW in the M_1 region compared to the patient's age $p \geq 0.05$.

Region M₂

The data analysis did not show a statistically significant difference in the size of SBH and SBW and MSW in the M_2 region compared to the patient's age $p \geq 0.05$.

3.2.1.3. Analysis by the size of the defect and the position of the missing teeth.

The obtained and analyzed data for the three criteria SBH, SBW and MSW in relation to the size of the defect and missing teeth position in it are shown in table 5.

	Researched criteria, mm	n area	Defect size	Mean	SD	Median	Q_1	Q_3	IQR	Range	Min	Max	t	ANOVA F	Kruskal Wallis	P
region PM_1	SBH	4	PM_1-M_1	x	x	x	x	x	x	x	x	x	x	x	x	x
		37	PM_1- M_2	11,07	3,34	x	x	x	x	12,90	4,31	17,21				
	SBW	4	PM_1-M_1	x	x	x	x	x	x	x	x	x	x	x	x	x
		37	PM_1- M_2	6,15	2,15	x	x	x	x	7,34	2,33	9,67				
	MSW	1	PM_1-M_1	x	x	x	x	x	x	x	x	x	x	x	x	x
		7	PM_1- M_2	5,86	2,28	x	x	x	x	6,00	3,40	9,40				
region PM_2	SBH	7	PM_2- M_1	x	x	6,00	5,41	6,60	1,19	4,00	2,80	6,80	x	x	0,36	0,948
		4	PM_1-M_1	x	x	x	x	x	x	x	x	x				
		23	PM_2- M_2	x	x	6,12	4,60	6,75	2,15	16,54	2,00	18,54				
		35	PM_1- M_2	x	x	6,23	4,40	8,00	3,60	9,30	1,61	10,91				
	SBW	7	PM_2- M_1	6,23	1,42	5,60	4,80	7,81	3,01	3,40	4,60	8,00	x	x	3,46	0,325
		4	PM_1-M_1	x	x	x	x	x	x	x	x	x				
		23	PM_2- M_2	6,74	2,00	6,28	4,80	8,41	3,61	7,00	3,40	10,40				
		35	PM_1- M_2	5,89	2,18	5,80	4,60	7,30	2,70	9,81	1,80	11,61				
	MSW	7	PM_2- M_1	6,94	1,96	7,21	4,80	9,00	4,20	5	4	9	x	x	0,013	1
		4	PM_1-M_1	x	x	x	x	x	x	x	x	x				
		19	PM_2- M_2	7,58	2,95	7,00	5,40	8,42	3,02	10,58	3,42	14,00				
		25	PM_1- M_2	7,22	2,24	7,60	5,40	8,02	2,62	10,77	2,83	13,6				
region M_1	SBH	8	M_1	4,38	1,32	4,60	3,30	5,56	2,26	3,60	2,20	5,80	x	x	19,1	0,002
		7	PM_2- M_1	4,49	1,24	4,22	3,40	5,61	2,21	3,20	3,00	6,20				
		31	M_1-M_2	4,09	1,50	4,20	3,00	5,40	2,40	5,60	1,20	6,80				
		4	PM_1-M_1	x	x	3,20	1,70	5,30	3,60	x	x	x				
		23	PM_2- M_2	x	x	2,60	1,80	3,20	1,40	5,05	1,20	6,25				
		35	PM_1- M_2	2,91	1,28	2,60	2,00	3,61	1,61	5,00	1,00	6,00				
	SBW	8	M_1	6,65	1,67	6,20	5,86	8,40	2,55	5,00	3,80	8,80	x	x	2,36	0,798
		7	PM_2- M_1	7,49	1,94	7,20	5,60	9,40	3,80	5,40	5,20	10,60				
		31	M_1-M_2	6,98	1,91	6,81	6,20	8,00	1,80	9,40	3,40	12,80				
		4	PM_1-M_1	x	x	x	x	x	x	x	x	x				
		23	PM_2- M_2	7,22	2,39	7,00	5,60	9,20	3,60	9,20	3,00	12,20				
		35	PM_1- M_2	6,88	3,43	6,55	4,00	8,20	4,20	11,40	2,60	14,00				
	MSW	8	M_1	10,1	1,08	10,10	9,25	11,16	1,91	3,00	8,40	11,40	x	x	6,71	0,243
		7	PM_2- M_1	10,38	1,49	10,21	9,20	11,41	2,21	4,59	8,41	13,00				
		31	M_1-M_2	10,61	3,06	9,80	8,40	13,00	4,60	12,00	5,80	17,80				
		4	PM_1-M_1	x	x	x	x	x	x	x	x	x				
		23	PM_2- M_2	11,30	2,64	11,20	9,21	12,80	3,59	10,40	7,40	17,80				
		35	PM_1- M_2	11,90	2,85	11,60	10,00	13,00	3,00	11,20	8,00	19,20				
region M_2	SBH	31	M_1-M_2	3,61	1,47	x	x	x	x	5,80	1,00	6,80	x	1,43	x	0,243
		23	PM_2- M_2	4,10	1,83	x	x	x	x	5,40	1,60	7,00				
		35	PM_1- M_2	3,32	1,83	x	x	x	x	6,60	1,00	7,60				
	SBW	31	M_1-M_2	8,61	2,56	x	x	x	x	10,20	4,80	15,00	x	0,45	x	0,639
		23	PM_2- M_2	8,85	2,64	x	x	x	x	9,60	4,00	13,60				
		35	PM_1- M_2	8,17	3,07	x	x	x	x	11,00	3,00	14,00				
	MSW	31	M_1-M_2	11,16	3,04	x	x	x	x	12,20	6,20	18,40	x	0,88	x	0,416
		23	PM_2- M_2	10,95	2,80	x	x	x	x	12,40	6,00	18,40				
		35	PM_1- M_2	11,91	2,99	x	x	x	x	12,20	6,60	18,80				

Table 5. Data for the three criteria SBH, SBW and MSW in relation to the size of the defect and missing teeth position in it

Region PM_1

It is impossible to analyze the data due to the small number of cases falling into the studied region PM_1-M_1.

Region PM_2

The data analysis does not show a statistically significant difference in the size of SBH and SBW and MSW in the PM_2 region compared to the size of the edentulous defect and the position of the missing teeth in it $p \geq 0.05$. The data analysis does not include the data for the region PM_2 in an edentulous defect in the region PM_1-M_1 due to the low number of cases.

Region M_1

Due to the low number of cases, the data analysis does not include data from region M_1 in an edentulous defect in region PM_1-M_1. The analysis of the data shows a statistically significant difference in the size of the SBH in region M_1 compared to the size of the edentulous defect and the position of the missing teeth in it $p \leq 0.05$. However, there was no statistically significant difference in the size of SBW and MSW in area M_1 compared to the size of the edentulous defect and the position of the missing teeth in it $p \geq 0.05$.

Region M_2

The data analysis does not show a statistically significant difference in SBH and SBW and MSW in region M_2 compared to the size of the edentulous defect and the position of the missing teeth in it $p \geq 0.05$.

3.2.1.4. Summary analysis and correlations

In conclusion a Kruskal–Wallis analysis was performed on the mean values of the data for the regions PM_1, PM_2, M_1 and M_2, which are shown in table 6. It shows that SBH decreased from the premolar to the molar area (Figure 28), and SBW and MSW increased from the premolar to the molar area (Figure 29 and 30) $p<0,0001$.

Researched criteria, mm	n area	Region	Mean
SBH	39	PM_1	10,80
	69	PM_2	6,18
	108	M_1	3,48
	89	M_2	3,62
SBW	39	PM_1	6,27
	69	PM_2	6,28
	108	M_1	7,07
	89	M_2	8,50
MSW	8	PM_1	5,98
	55	PM_2	7,35
	108	M_1	11,18
	89	M_2	11,40

Table 6. Mean values of date for the regions PM_1, PM_2, M_1 M_2

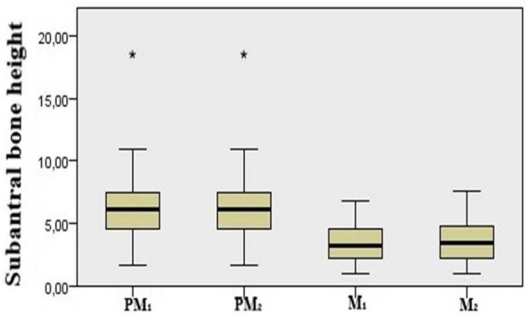

Figure 28 Box plot mean values of SBH for the regions PM_1, PM_2, M_1, M_2.

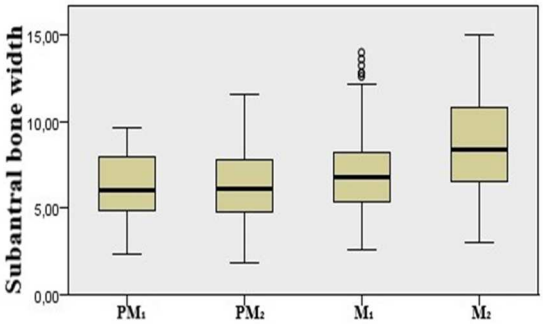

Figure 29. Box plot mean values of SBW for the regions PM1, PM2, M1,M2

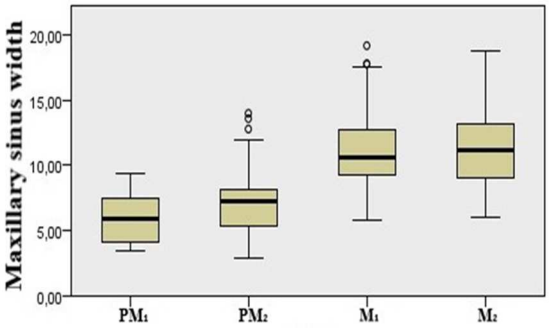

Figure 30. Box plot mean values of MSW for the regions PM1, PM2, M1, M2

After the complete analysis of the data from the regions PM1, PM2, M1 и M2, significant inverse reation was found between MSW and SBH p<0,01. Between MSW and SBW, there was a significant direct relation p<0.01. They are shown in table 7.

Researched criteria		**SBH**	**SBW**
MSW	r	-,576**	,287**
	P	0,000	0,000
	N	260	260

Table 7. Complete analysis

3.2.2. Results for task 2.

3.2.2.1 Analysis according to operators by method for the application of implants in conditions of subantral deficiency MSFALAIIP and MSFALADIP.

Data on the SBH in millimeters according to operators by method of the application of implants in conditions of subantral deficiency and their analysis are shown in table 8.

Implant application method	N	Operator	Mean	SD	Median	Q_1	Q_3	IQR	Range	Min	Max	Kruskal Wallis	P
MSFALAIIP	38	*1*	3,75	1,53	3,60	2,55	5,00	2,45	5,60	1,20	6,80	10, 036	0,018
	28	*2*	4,43	1,16	4,50	3,30	5,40	2,10	4,25	2,00	6,25		
	22	*3*	4,09	1,52	3,71	2,90	5,45	2,55	5,40	1,40	6,80		
	12	*4*	5,27	1,28	5,70	4,28	6,35	2,07	3,80	3,00	6,80		
MSFALADIP	0	*1*	x	x	x	x	x	x	x	x	x	x	x
	30	*2*	3,13	1,65	2,40	2,00	3,86	1,86	5,80	1,00	6,80	0,196	0,907
	24	*3*	3,34	2,04	2,51	1,61	5,58	3,97	5,75	1,00	6,75		
	7	*4*	3,26	1,59	2,80	2,00	4,22	2,22	4,60	1,80	6,40		

Table 8. The data on the SBH in millimeters and the result of their analysis according to operators according to the method of applying implants in conditions of subantral deficiency

The data analysis shows a statistically significant difference in the size of the SBH compared to the MSFALAIIP method for the four operators $p \leq 0.05$. In the analysis of the data on the height of the SBH in relation to the MSFALADIP method, operator 1 is excluded, since there is no data that he applies this method. For operator 2, 3 and 4, no statistically significant difference was observed in the sizes of the height of the SBH compared to the MSFALADIP method $p \geq 0.05$

3.2.2.2 Analysis by method for the application of implants in conditions of subantral deficiency MSFALAIIP and MSFALADIP by operators.

The data on the SBH in millimeters according to the method for the application of implants in conditions of subantral deficiency

MSFALAIIP and MSFALADIP by operators and their analysis are shown in table 9.

Operator	N	Implant application method	Mean	SD	Median	Q_1	Q_3	IQR	Range	Min	Max	t	U	P
Operator 1	38	*MSFALAIIP*	3,75	1,53	3,60	2,55	5,00	2,45	5,60	1,20	6,8	x	x	x
	0	*MSFALADIP*	x	x	x	x	x	x	x	x	x			
Operator 2	28	*MSFALAIIP*	4,43	1,16	4,50	3,30	5,40	2,10	4,25	2,00	6,25	x	213,50	0,001
	30	*MSFALADIP*	3,13	1,65	2,40	2,00	3,86	1,86	5,80	1,00	6,80			
Operator 3	22	*MSFALAIIP*	4,09	1,52	3,71	2,90	5,45	2,55	5,40	1,40	6,80	x	189,00	0,099
	24	*MSFALADIP*	3,34	2,04	2,51	1,61	5,58	3,97	5,75	1,00	6,75			
Operator 4	12	*MSFALAIIP*	5,27	1,28	5,70	4,28	6,35	2,07	3,80	3,00	6,80	2,84771	x	0,01649
	7	*MSFALADIP*	3,26	1,59	2,80	2,00	4,22	2,22	4,60	1,80	6,40			

Table 9. Data on the SBH in millimeters according to the method for the application of implants in conditions of subantral deficiency MSFALAIIP and MSFALADIP by operators and their analysis

It is noticed that, the method for the application of implants in conditions of subantral deficiency MSFALAIIP, with operator 1 and 3 is in a wider range of the height of the HCK, respectively 5,60 mm and 5,40 mm, compared to operator 2 and 4 - 4.25 mm and 3,80 mm. The extended range of the SBH in operator 1 and 3 is a result of the lower minimum value of the SBH when applying MSFALAIIP – 1,20 mm and 1,40 mm, respectively, compared to operator 2 and 4 – 2,00 mm and 3,00 mm (Figure 34).

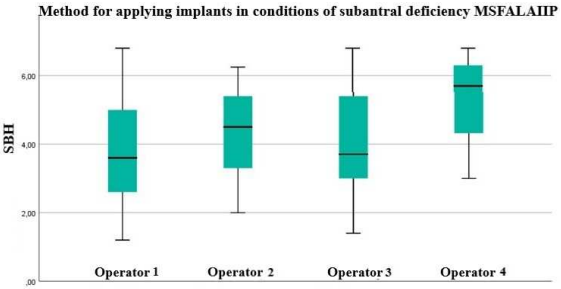

Figure 31. Box plot of SBH, in which operators undertake MSFALAIIP

The data analysis for operator 2 and 4 shows a statistically significant difference in the size of the SBH compared to the method of applying implants in conditions of subantral deficiency MSFALAIIP and MSFALADIP $p \leq 0.05$. In operator 3, no statistically significant difference was observed in the size of the SBH compared to the method of applying implants in conditions of subantral deficiency MSFALAIIP and MSFALADIP $p \geq 0.05$. Operator 1 is excluded from the analysis because he/she only applies the MSFALAIIP method in solving his/her clinical cases.

3.2.3. Results for task 3.

SV data of MSF total surface area are visible in table 10.Thirty-one observations were not included in the data analysis due to zero SV of MSF total observation area. This zero visibility was observed at the medial, central and distal openings with an endoscope penetration of 20 mm and a viewing angle with the endoscope of 15°. For medial are 9, for central - 8 and for distal - 14

Opening	Depth	Angle	n	Mean	SD	Max	Min	Range	Median	Q_1	Q_3	IQR
Medial	10 mm	45°	40	0,12	0,02	0,18	0,08	0,10	0,12	0,11	0,14	0,03
Central	10 mm	45°	40	0,12	0,02	0,18	0,07	0,10	0,11	0,10	0,13	0,03
Distal	10 mm	45°	40	0,12	0,02	0,16	0,08	0,08	0,11	0,10	0,13	0,03
Distal	20 mm	90°	40	0,10	0,02	0,14	0,05	0,10	0,10	0,08	0,11	0,03
Central	20 mm	90°	40	0,09	0,02	0,11	0,04	0,07	0,09	0,08	0,10	0,02
Medial	20 mm	45°	40	0,08	0,02	0,12	0,03	0,09	0,08	0,07	0,10	0,03
Medial	20 mm	90°	40	0,08	0,02	0,14	0,04	0,10	0,08	0,07	0,09	0,02
Distal	10 mm	90°	40	0,08	0,02	0,12	0,03	0,09	0,08	0,07	0,09	0,02
Central	20 mm	45°	40	0,07	0,02	0,11	0,03	0,08	0,07	0,06	0,09	0,03
Central	10 mm	90°	40	0,07	0,02	0,12	0,03	0,09	0,07	0,05	0,08	0,03
Distal	20 mm	45°	40	0,07	0,02	0,11	0,02	0,09	0,07	0,04	0,09	0,05
Medial	10 mm	15°	40	0,07	0,03	0,13	0,02	0,12	0,06	0,04	0,09	0,05
Medial	10 mm	90°	40	0,06	0,02	0,10	0,02	0,08	0,07	0,04	0,08	0,04
Central	10 mm	15°	40	0,06	0,02	0,11	0,01	0,10	0,05	0,04	0,07	0,03
Distal	10 mm	15°	40	0,04	0,02	0,09	0,01	0,08	0,04	0,03	0,05	0,02
Medial	20 mm	15°	31	0,04	0,02	0,08	0,01	0,08	0,04	0,02	0,05	0,03
Central	20 mm	15°	32	0,03	0,02	0,06	0,00	0,06	0,03	0,02	0,04	0,02
Distal	20 mm	15°	26	0,02	0,01	0,05	0,00	0,05	0,02	0,01	0,03	0,02

Table 10. The obtained data for SV of the total area when observing MSF for medial, central and distal opening with penetration depth of 10mm and 20mm

3.2.3.1. Data analysis to endoscopic access opening

The analysed data for SV of MSF total field of view to the endoscopic access opening are shown in table 11.

Opening	Depth	Angle	n	Mean	SD	Median	Q_1	Q_3	IQR	Range	Min	Max	ANOVA F	Kruskal Wallis	P
Medial	10 mm	15°	40	0,07	0,03	0,06	0,04	0,09	0,05	0,12	0,02	0,13		15,25	0,000
Central			40	0,06	0,02	0,05	0,04	0,07	0,03	0,10	0,01	0,11			
Distal			40	0,04	0,02	0,04	0,03	0,05	0,02	0,08	0,01	0,09			
Medial	20 mm	15°	31	0,04	0,02	0,04	0,02	0,05	0,03	0,08	0,01	0,08	6 327 080		0,00246
Central			32	0,03	0,02	0,03	0,02	0,04	0,02	0,06	0,00	0,06			
Distal			26	0,02	0,01	0,02	0,01	0,03	0,02	0,05	0,00	0,05			
Medial	10 mm	45°	40	0,12	0,02	0,12	0,11	0,14	0,03	0,10	0,08	0,18	1,974228		0,143468
Central			40	0,12	0,02	0,11	0,10	0,13	0,03	0,08	0,08	0,16			
Distal			40	0,12	0,02	0,11	0,10	0,13	0,03	0,10	0,07	0,18			
Medial	20 mm	45°	40	0,08	0,02	0,08	0,07	0,10	0,03	0,09	0,03	0,12	6,486057		0,002131
Central			40	0,07	0,02	0,07	0,06	0,09	0,03	0,08	0,03	0,11			
Distal			40	0,07	0,02	0,07	0,04	0,09	0,05	0,09	0,02	0,11			
Medial	10 mm	90°	40	0,06	0,02	0,07	0,04	0,08	0,04	0,08	0,02	0,10	6,606755		0,001912
Central			40	0,07	0,02	0,07	0,05	0,08	0,03	0,09	0,03	0,12			
Distal			40	0,08	0,02	0,08	0,07	0,09	0,02	0,09	0,03	0,12			
Medial	20 mm	90°	40	0,08	0,02	0,08	0,07	0,09	0,02	0,10	0,04	0,14		15,25	0,000
Central			40	0,09	0,02	0,09	0,08	0,10	0,02	0,07	0,04	0,11			
Distal			40	0,10	0,02	0,10	0,08	0,11	0,03	0,10	0,05	0,14			

Table 11. SV data from the total observation area of MSF and the result of its analysis relative to the endoscopic access port

There was no statistically significant difference in SV of MSF total field of view relative to the medial, central, and distal endoscopic access openings at an endoscope penetration of 10 mm and an endoscope viewing angle of 45°, $p \geq 0.05$. SV of MSF total field of view was the same for all three openings, and this SV was the highest compared with all other observations performed.

From the data analysis, there was a statistically significant difference in SV of the total field of view MSF from the medial, central and distal openings at an endoscope penetration of 10 mm and an viewing angle with the endoscope of 15° - $p \leq 0.05$, with SV of the total field of view of MSF decreasing from the medial (0.07 ± 0.03) to the distal opening (0.04 ± 0.02).

There was a statistically significant difference in the share of the total field of view of MSF to the medial, central, and distal openings at an endoscope penetration of 20 mm and an endoscope viewing angle of 15° - $p \leq 0.05$, with the share of the total field of view of MSF decreasing from the medial (0.04 ± 0.02) to the distal opening (0.02 ± 0.01).

There was a statistically significant difference in the share of the total field of view of MSF to the medial, central, and distal openings at an endoscope penetration of 20 mm and an endoscope viewing angle of 45°, $p \leq 0.05$, with the share of the total field of view of MSF decreasing from the medial (0.08 ± 0.02) to the distal opening (0.07 ± 0.02).

There was a statistically significant difference in the share of the total field of view of MSF to the medial, central, and distal openings at an endoscope penetration of 10 mm and an endoscope viewing angle of 90°, $p \leq 0.05$, with the share of the total field of view of MSF increasing from the medial (0.06 ± 0.02) to the distal opening (0.08 ± 0.02).

There was a statistically significant difference in the share of the total field of view of MSF to the medial, central and distal openings at an endoscope penetration of 20 mm and an endoscope viewing angle of 90° - $p \leq 0.05$, with the share of the total field of view of MSF increasing from the medial (0.08 ± 0.02) to the distal opening (0.10 ± 0.02).

3.2.3.2. Data analysis to endoscope penetration depth

The analysed data for SV of total field of view of MSF to the depth of endoscope penetration are shown in table 12.

Depth	Opening	Angle	n	Mean	SD	Median	Q_1	Q_3	IQR	Range	Min	Max	t test	Wilcoxon	P
10 mm	Medial	15°	40	0,07	0,03	0,06	0,04	0,09	0,05	0,12	0,02	0,13	10,374992		0,000
20 mm			31	0,04	0,02	0,04	0,02	0,05	0,03	0,08	0,01	0,08			
10 mm	Central	15°	40	0,06	0,02	0,05	0,04	0,07	0,03	0,10	0,01	0,11	9,326934		0,000
20 mm			32	0,03	0,02	0,03	0,02	0,04	0,02	0,06	0,00	0,06			
10 mm	Distal	15°	40	0,04	0,02	0,04	0,03	0,05	0,02	0,08	0,01	0,09		4,38	0,000
20 mm			26	0,02	0,01	0,02	0,01	0,03	0,02	0,05	0,00	0,05			
10 mm	Medial	45°	40	0,12	0,02	0,12	0,11	0,14	0,03	0,10	0,08	0,18	11,796176		0,000
20 mm			40	0,08	0,02	0,08	0,07	0,10	0,03	0,09	0,03	0,12			
10 mm	Central	45°	40	0,12	0,02	0,11	0,10	0,13	0,03	0,08	0,08	0,16	14,051088		0,000
20 mm			40	0,07	0,02	0,07	0,06	0,09	0,03	0,08	0,03	0,11			
10 mm	Distal	45°	40	0,12	0,02	0,11	0,10	0,13	0,03	0,10	0,07	0,18	12,458648		0,000
20 mm			40	0,07	0,02	0,07	0,04	0,09	0,05	0,09	0,02	0,11			
10 mm	Medial	90°	40	0,06	0,02	0,07	0,04	0,08	0,04	0,08	0,02	0,10		3,97	0,000
20 mm			40	0,08	0,02	0,08	0,07	0,09	0,02	0,10	0,04	0,14			
10 mm	Central	90°	40	0,07	0,02	0,07	0,05	0,08	0,03	0,09	0,03	0,12	5,97		0,000
20 mm			40	0,09	0,02	0,09	0,08	0,10	0,02	0,07	0,04	0,11			
10 mm	Distal	90°	40	0,08	0,02	0,08	0,07	0,09	0,02	0,09	0,03	0,12	4,87		0,000
20 mm			40	0,10	0,02	0,10	0,08	0,11	0,03	0,10	0,05	0,14			

Table 12. The SV data from the total observation area of MSF and the result of its analysis against the depth of penetration of the endoscope

There was a statistically significant difference of SV of the total field of view of MSF in the medial opening at an endoscope viewing angle of 15° to endoscope penetration depth of 10 and 20 mm, respectively, $p \leq 0.05$, with SV of the total field of view of MSF decreasing from 10 (0.07 ± 0.03) to 20 mm (0.04 ± 0.02) endoscope penetration depth.

There was a statistically significant difference in the share of the total field of view of MSF in the central opening at an endoscope viewing angle of 15° to endoscope penetration depth of 10 and 20 mm, respectively, $p \leq 0.05$, with SV of the total field of view of MSF decreasing from 10 (0.06 ± 0.02) to 20 mm (0.03 ± 0.02) endoscope penetration depth.

There was a statistically significant difference in the share of the total field of view of MSF in the distal opening at an endoscope viewing angle of 15° to endoscope penetration depth of 10 and 20 mm, respectively, $p \leq 0.05$, with SV of the total field of view of MSF decreasing from 10 (0.04 ± 0.02) to 20 mm (0.02 ± 0.01) endoscope penetration depth.

There was a statistically significant difference in the share of the total field of view of MSF in the medial opening at an endoscope viewing angle of 45° to endoscope penetration depth of 10 and 20 mm, respectively, $p \leq 0.05$, with SV of the total field of view of MSF decreasing from 10 (0.12 ± 0.02) to 20 mm (0.08 ± 0.02) endoscope penetration depth.

There was a statistically significant difference in the share of the total field of view of MSF in the central opening at an endoscope viewing angle of 45° to endoscope penetration depth of 10 and 20 mm, respectively, $p \leq 0.05$, with SV of the total field of view of MSF decreasing from 10 (0.12 ± 0.02) to 20 mm (0.07 ± 0.02) endoscope penetration depth.

There was a statistically significant difference in the share of the total field of view of MSF in the distal opening at an endoscope viewing angle of 45° to endoscope penetration depth of 10 and 20 mm, respectively, $p \leq 0.05$, with SV of the total field of view of MSF decreasing from 10 (0.12 ± 0.02) to 20 mm (0.07 ± 0.02) endoscope penetration depth.

SV of the total field of view of MSF to the 10 mm depth of penetration was constant for all three endoscopic access holes at a 45° endoscope viewing angle, whereas the share of the total field of view of MSF to the 20 mm depth of penetration decreased from medial (0.08 ± 0.02) to distal (0.07 ± 0.02).

There was a statistically significant difference in the share of the total field of view of MSF in the medial opening at an endoscope viewing angle of 90° to endoscope penetration depth of 10 and 20 mm,

respectively, $p \leq 0.05$, with SV of the total field of view of MSF decreasing from 10 (0.06 ± 0.02) to 20 mm (0.08 ± 0.02) endoscope penetration depth.

There was a statistically significant difference in the share of the total field of view of MSF in the central opening at an endoscope viewing angle of 90° to endoscope penetration depth of 10 and 20 mm, respectively, $p \leq 0.05$, with SV of the total field of view of MSF increasing from 10 (0.07 ± 0.02) to 20 mm (0.09 ± 0.02) endoscope penetration depth.

There was a statistically significant difference in the share of the total field of view of MSF in the distal opening at an endoscope viewing angle of 90° to endoscope penetration depth of 10 and 20 mm, respectively, $p \leq 0.05$, with SV of the total field of view of MSF increasing from 10 (0.08 ± 0.02) to 20 mm (0.10 ± 0.02) endoscope penetration depth.

3.2.3.3. Analysis of the data to the viewing angle with the endoscope

The analysed data for SV of the total field of view of the maxillary sinus to the viewing angle with the endoscope are shown in table 13.

Angle	Opening	Depth	n	Mean	SD	Median	Q_1	Q_3	IQR	Range	Min	Max	ANOVA F	Fridman	P
15°	Medial	10 mm	40	0,07	0,03	0,06	0,04	0,09	0,05	0,12	0,02	0,13			
45°			40	0,12	0,02	0,12	0,11	0,14	0,03	0,10	0,08	0,18			
90°			40	0,06	0,02	0,07	0,04	0,08	0,04	0,08	0,02	0,10	80,54702		0,000
15°	Medial	20 mm	31	0,04	0,02	0,04	0,02	0,05	0,03	0,08	0,01	0,08			
45°			40	0,08	0,02	0,08	0,07	0,10	0,03	0,09	0,03	0,12			
90°			40	0,08	0,02	0,08	0,07	0,09	0,02	0,10	0,04	0,14		42	0,000
15°	Central	10 mm	40	0,06	0,02	0,05	0,04	0,07	0,03	0,10	0,01	0,11			
45°			40	0,12	0,02	0,11	0,10	0,13	0,03	0,08	0,08	0,16			
90°			40	0,07	0,02	0,07	0,05	0,08	0,03	0,09	0,03	0,12	83,44512		0,000
15°	Central	20 mm	32	0,03	0,02	0,03	0,02	0,04	0,02	0,06	0,00	0,06			
45°			40	0,07	0,02	0,07	0,06	0,09	0,03	0,08	0,03	0,11			
90°			40	0,09	0,02	0,09	0,08	0,10	0,02	0,07	0,04	0,11	131,6742		0,000
15°	Distal	10 mm	40	0,04	0,02	0,04	0,03	0,05	0,02	0,08	0,01	0,09			
45°			40	0,12	0,02	0,11	0,10	0,13	0,03	0,10	0,07	0,18			
90°			40	0,08	0,02	0,08	0,07	0,09	0,02	0,09	0,03	0,12		60	0,000
15°	Distal	20 mm	26	0,02	0,01	0,02	0,01	0,03	0,02	0,05	0,00	0,05			
45°			40	0,07	0,02	0,07	0,04	0,09	0,05	0,09	0,02	0,11			
90°			40	0,10	0,02	0,10	0,08	0,11	0,03	0,10	0,05	0,14	166,7588		0,000

Table 13. Data for SV of the total field of view of the maxillary sinus to the viewing angle with the endoscope.

There was a statistically significant difference in SV of the total field of view of MSF for medial opening and endoscope penetration depth of 10 mm to viewing angle of 15°, 45°, and 90°, respectively, $p \leq 0.05$, with the highest share of visibility observed at a viewing angle of 45° (0.12 ± 0.02) and the lowest share at 90° (0.06 ± 0.02).

There was a statistically significant difference in SV of the total field of view of MSF for medial opening and endoscope penetration depth of 20 mm to viewing angle of 15°, 45° and 90°, respectively - $p \leq 0.05$, with SV increasing from viewing angle of 15° (0.04 ± 0.02) to 90° (0.08 ± 0.02).

There was a statistically significant difference in SV of the total field of view of MSF for a central opening and 10 mm endoscope

penetration depth to viewing angle of 15°, 45° and 90°, respectively, $p \leq 0.05$, with the highest share of visibility observed at an viewing angle of 45° (0.12 ± 0.02) and the lowest share at 15° (0.06 ± 0.02).

There was a statistically significant difference in SV of the total field of view of MSF for central opening and endoscope penetration depth of 20 mm to viewing angle of 15°, 45° and 90°, respectively $p \leq 0.05$, with SV increasing from viewing angle of 15° (0.03 ± 0.02) to 90° (0.09 ± 0.02).

There was a statistically significant difference in SV of the total field of view of MSF for distal opening and endoscope penetration depth of 10 mm to viewing angle of 15°, 45° and 90°, respectively $p \leq 0.05$, with the highest SV observed at viewing angle of 45° (0.12 ± 0.02) and the lowest share at 15° (0.04 ± 0.02).

There was a statistically significant difference of SV of the total field of view of MSF for distal opening and 20 mm endoscope penetration depth to viewing angle of 15°, 45° and 90°, respectively $p \leq 0.05$, with SV increasing from viewing angle of 15° (0.02 ± 0.01) to 90° (0.10 ± 0.02).

3.2.4. Results for task 4.

The data obtained for operator fatigue and machine execution time for the osteotomy technique and trocar-guided endoscopic approach technique and their analysis is presented in table 14.

Researched criterion	n	Technique	Mean	SD	Median	Q_1	Q_3	IQR	t	U test	P
Time in sec.	12	*Machine osteotomy*	93,08	15,11	95,00	80,5	108,25	27,75	x	132	0
	11	*Trocar guided*	231,91	58,66	273,00	187	279	92			
Fatigue	12	*Machine osteotomy*	2,83	1,59	2,50	1,25	4,75	3,5	-6,2	x	0,000004
	11	*Trocar guided*	7,27	1,85	7,00	5	9	4			

Table 14. data on operator fatigue and machine run time osteotomy technique and trocar-guided technique for endoscopic access and the result of their analysis

Data analysis showed a statistically significant difference in operator fatigue and time to perform endoscopic approach with the machine osteotomy technique compared to the performance of the trocar-guided technique - $p \leq 0.05$.

Ensuring endoscopic approach using the trocar-guided technique is a difficult task to perform from a clinical point of view, especially when the anterior wall of the maxillary sinus is thicker. The resulting endoscopic approach opening with the trocar-guided technique is larger compared to that obtained with the machine osteotomy technique.

It was expected that in the trocar-guided technique, the cannula used because of its fenestrated tip would contribute to less blood staining of the endoscope camera, which in turn would improve visibility during MSFALA. Visibility is the same when using both cannulas.

The use of the trocar-guided technique does not provide any advantages over the machine osteotomy technique.

3.3. DISCUSSION

3.3.1. Discussion for task 1.

There is a proportional relationship between the number of bone defect walls involved in the augmentation process and the number of osteogenic cells available (42, 81, 139).

MSFA is the most commonly used procedure for the permanent creation of the necessary level of the subantral bone for the placement of dental implants with a conventional length of 8 mm in the distal parts of the maxilla. The procedure has been used for almost 40 years in implant surgery and has high predictability for the success of implant treatment (152, 166).

Factors that favor the success of the maxillary sinus floor augmentation are still under discussion (69).

In recent years, attention has been paid to the morphology of the MS and, in particular, its width in the vestibular-palatal direction, taking into account the distance between the medial and lateral walls of the maxillary sinuses. In addition, attempts have been made to develop a classification of MS to support the preoperative planning of the augmentation procedure to choose an approach suitable for bone repair material (48, 159).

Bertl et. al. (24) argue that MSW is a relevant factor for graft consolidation in MSFA. They investigated the possibility of compiling an accessible and clinically relevant classification of MS based on its width in the vestibular-palatal direction, taking into account the distance between the medial and lateral walls of MS. Still, due to the large variation of MSW, the authors conclude that the creation of an accessible and meaningful classification of MS is not possible. They found that MSW in the vestibular-palatal direction was associated with SBW and SBH.

Several publications report an inverse relationship between the percentage of newly formed bone after the MSFA augmentation procedure and its width, taking into account the distance between the

medial and lateral walls of the MS in the vestibular-lateral ridge of the alveolar ridge (15, 102, 147, 148).

To prepare a specification for subantral deficiency, 76 preoperative CBCTs were considered in patients with MSFA augmentation procedure with lateral approach, and a total of 108 MS were monitored, with a total of 305 missing teeth identified. On each of the 305 missing teeth the parameters SBH, SBW, and MSW were measured. The latter parameter was selected to be measured at 8 mm from the ridge of the alveolar ridge, according to the literature, for an inversely proportional relationship between the percentage of newly formed bone after the MSFA augmentation procedure and its width (15, 102, 147, 148), also we took into account the fact that this is the minimum height required for the placement of a conventional length implant.

3.3.2. Discussion for task 2.

Bhandari et al. (25) in a clinical study of 10 patients reported a sinus floor elevation with lateral approach and immediate implant placement at a height of 4-6 mm of SBH.

Tukel et al. (165) in a retrospective study in the period from March 2015 - September 2016, at the Department of Oral and Maxillofacial Surgery, Faculty of Dentistry, Cukurova University, Turkey, reported performing lateral approach sinus floor elevation and immediate implant placement in 120 patients. The height of available subantral bone of the patients varied from 3 – 6 mm.

Barbu et al. (17) in a clinical study of 14 patients in the period from October 2013 - July 2014 reported on the lifting of the sinus floor with lateral approach and immediate placement of an implant at a SBH 4 - 5 mm.

De Souza et al. (57) reported on the attempted and performed elevation of the sinus floor with a lateral approach and immediate placement of an implant in the upper right first molar region of a female patient, with a SBH of 3.5 mm.

Valentini et al. (168) in a clinical study of 56 patients reported sinus floor elevation with lateral approach performed and immediate implant placement at a mean SBH 2.1 mm

D'Elia et al. (53) in a systematic review stated that elevation of the sinus floor with lateral approach and immediate implant placement can be used to treat patients with an atrophic maxilla with a SBH 1-3 mm, in cases, when initial stability of the implants can be achieved.

In the literature today, a trend is noticed that the SBH at which the method for the application of implants in conditions of subantral deficiency MSFALAIIP is undertaken acquires a wider range. This is due to the lower reported minimum value of the SBH at which MSFALAIIP is undertaken - 1-2 mm, but only in cases where initial stability of the implants can be achieved. This same trend is observed in the clinical cases of operator 1 and 3, who undertake MSFALAIIP at a SBH 1-2 mm.

3.3.3. Discussion for task 3.

Pashkova et. al. (126) in a clinical case of implant placement, reported the use of a 3D CBCT-based printed model of the patient, which helps to pre-visualize the surgical field, thereby improving preoperative preparation and selection of the most accurate approach in treatment planning.

Georgantza et. al. (72) in a report discussed the basic principles and applications of 3D printed models based on CBCT data of patients for training in dental implantology. The authors stated that there are 3 main applications of 3D printed models in dental implantology training - for better illustration in teaching anatomical structures, treatment planning and preoperative practice, and with simulation applications. They conclude that 3D printed models based on CBCT data of patients have great potential for implantology education, for better understanding and planning of surgical manipulations.

Tuce et. al. (164) explored the possibility of simulating a maxillary sinus floor lifting procedure on 3D printed models based on CBCT data of patients. The study resulted in the augmentation of the maxillary sinus floor and the placement of an implant on the 3D printed model, which served as a simulator of the operative field to train the operator's practical skills. The authors conclude that the 3D printed models could serve as simulation materials for training, and in dental practice for treatment planning.

Araneda et. al. (10) conducted a study to present a strategy for morphological analysis of the maxillary sinus using 3D printed models, based on CBCT data of patients. 24 patients were included. A total of 48 models were produced. The authors concluded that 3D printed models provide a new approach to understand the exact anatomical characteristics of the maxillary sinus, compared to its evaluation on a two-dimensional screen. 3D printed maxillary sinus models are a suitable method for preoperative analysis and training.

Meglioli et. al. (107) in a systematic literature review aimed to evaluate the use of 3D printed bone models for training, simulation and/or intervention planning in oral and maxillofacial surgery. As a result, they found that 3D printed bone models are mainly used as training or simulation models in bone reconstruction. FDM 3D printers showed satisfactory results for creating training models.

With our study, we confirm that FDM 3D printed simulation models based on CBCT images reproduce anatomical features in detail and serve as a simulator of the surgical field to train the operator's manual skills, the materialized visualization of the surgical field provides an opportunity to find the most accurate approach in the preoperative preparation of a clinical case. Our presented 3D printing algorithm can be useful for the production of accessible training materials. There are not many reports in the literature focusing on dental implantology using endoscopically guided augmentation procedure to lift the MSF by using endoscopes with angled visual axis

0°, 30°, 45°, 70°, 90°, and 120° deviated from the instrument axis. The authors point to the endoscopically assisted MSF augmentation procedure as a minimally invasive technique with good visual control of the operative field, allowing detection of intraoperative Schneiderian membrane perforations during manipulation (5, 21, 60, 67, 80, 117, 173). The literature describes the use of endoscopes with different angled visual axis in augmentation procedure of MSF lifting, but no studies were found to indicate the most optimal endoscopic approach with the highest SV of the total MSF area.

3.3.4. Discussion for task 4.

Köhler et al. (94) concluded that the endonasal approaches for the treatment of maxillary sinus disease described in otorhinolaryngology turn out to be inapplicable to the needs of dental implantology and more specifically when performing an endoscopically guided maxillary sinus floor elevation procedure, as they do not can provide a comprehensive optical, atraumatic and direct view of the floor of the maxillary sinus above Schneider's membrane. The authors claim that for the needs of dental implantology, approach through the fossa canina when performing an endoscopically navigated procedure to elevate the floor of the maxillary sinus is suitable, time-honored, but long-forgotten by otorhinolaryngologists.

Engelke et al. (61) suggestr special endoscopic techniques for the needs of dentistry that are comparable in many respects to the techniques used in otorhinolaryngology. They are direct endoscopy, immersion endoscopy, assisted endoscopy, assisted immersion endoscopy, trocar guided endoscopy. Trocar-guided endoscopy is performed in the center of the canine fossa and requires a puncture of the anterior wall of the maxillary sinus with a trocar. The formation of the resulting opening with a diameter of up to 5 mm provides a space between the floor of the maxillary sinus and Schneider's membrane and the endoscope, which is called the subantral space. The procedure is for direct endoscopic visualization, for the purpose of biopsies,

removal of foreign bodies, for evaluation of Schneider's membrane in case of suspected inflammation, identification and control of perforations of Schneider's membrane during its elevation during an augmentation procedure to elevate the floor of the maxillary sinus, as well as control of the positioning of the barrier membrane and bone repair material during an augmentation procedure on maxillary sinus floor elevation.

There is evidence in the literature of an endoscopically guided maxillary sinus floor elevation procedure with approach through the fossa canina, with the endoscopic approach opening being accomplished through a machine osteotomy.

Gandhi (151) in a clinical study of 20 patients undergoing an augmentation procedure for endoscopically guided maxillary sinus floor elevation and a total of 30 implants placed, aimed to evaluate the usefulness and applicability of endoscopic control during the procedure. Patients with residual subantral bone height between 2 mm and 5 mm were included in the study. Patients were divided into two groups. One included patients with a subantral bone height < 4 mm who underwent a maxillary sinus floor elevation procedure with a lateral approach, and the other group included patients with a subantral bone height > 4 mm who underwent a maxillary sinus floor elevation procedure using an osteotomy technique. In both groups, endoscopic control was performed through the fossa canina, using a Xuzhou Ikeda (China) endoscope with an angled visual axis of 45° or 70° deviated from the axis of the instrument. The three millimeter opening for the endoscopic approach is made by machine osteotomy, using a round surgical carbide bur.

Hu et al. (80) reported a clinical case in which the objective was to simultaneously remove an antral pseudocyst and perform an augmentation procedure to elevate the floor of the maxillary sinus through endoscopically guided surgery. For the endoscopic control, approach through the fossa canina and an endoscope with a visual axis

of 0° to the axis of the instrument were used. The opening for the endoscopic approach was made by machine osteotomy, using a piezoelectric surgical device (Piezosurgery, Silfradent, Italy). The opening measured 5 mm by 8 mm.

No data were found in the literature for a comparative evaluation between the machine osteotomy technique and the trocar otorhinolaryngology technique for creating an opening for endoscopic approach through the fossa canina.

4. CONCLUSION

It is not uncommon for a specialist in dental implantology in their practice to encounter severely deteriorated conditions for rehabilitation in the distal areas of the upper jaw, where the height of the available subantral bone is less than 3 mm. In our study, we found that the volume of available subantral bone does not depend on the gender and age of the patient, nor on the size of the edentulous defect. The height of the available subantral bone decreases from the premolar to the molar region, and the width of the available subantral bone and the width of the maxillary sinus increase from the molar to the premolar region. The only treatment option for such clinical cases remains the augmentation procedure of elevation of the sinus floor with lateral approach, which is a well-known and predictable procedure. There are two methods of implant placement in conditions of subantral deficiency – lateral approach sinus floor elevation with immediate implant placement and delayed implant placement. The advantages of the immediate implant placement method over the delayed one is that the placed implants serve to support the elevated sinus membrane and the placed bone restorative material. The implementation of the immediate placement of implants depends on achieving primary stability of the placed implants and the common typical complication – perforation of the elevated sinus

mucoperiosteum, which gives origin of the difficulty in the implementation of this method.

The optimization of the procedure can be carried out in two directions - in preoperative preparation and planning and the surgical technique of execution.

To optimize the sinus floor elevation procedure with lateral approach, we suggest the introduction of 3D anatomical simulation models to be included in the preoperative preparation and planning of the surgical manipulation, in order to understand the individual anatomy of certain objects, through their visualization, as well as to serve as a physical training object in the performance of specific surgical techniques to improve the operator's dexterity.

For the purpose of improving the surgical technique we suggest to introduce endoscopic control during the augmentation procedure. We have confirmed that for the needs of dental implantology when performing an endoscopically guided sinus floor elevation procedure, it is appropriate for the endoscopic approach to be performed via the fossa canina for direct endoscopic visualization to assess and control perforations of the Schneider's membrane during its elevation. The largest share of visibility of the total field of view of the sinus floor is achieved when the endoscope enters in an antero-posterior direction at 10 mm and an angle of observation of 45° at comparable 15°, 45° and 90°. The opening for endoscopic approach can be made by trocar-guided or machine-assisted osteotomy technique. We proved that the trocar-guided technique is a difficult task to perform, offers no advantages over the machine osteotomy technique, and endoscope visibility is the same for both approach opening techniques.

5. CONCLUSIONS

1. The volume of available subantral bone does not depend on the sex and age of the patient, nor on the size of the edentulous defect.

2. The height of the available subantral bone decreases from the premolar to the molar region, and the width of the available subantral bone and the width of the maxillary sinus increase from the molar to the premolar region.

3. A significant inverse relationship was found between the width of the maxillary sinus and the height of the available subantral bone, and a significant direct relationship was observed between the width of the maxillary sinus and the width of the available subantral bone.

4. The height of the available subantral bone is a factor in undertaking an implant placement method in the setting of subantral deficiency in maxillary sinus floor augmentation with lateral approach with immediate implant placement, but not for maxillary sinus floor augmentation with lateral approach with delayed placement of implants.

5. The height of the available subantral bone in which maxillary sinus floor augmentation with lateral approach is undertaken with immediate implant placement acquires a wider range due to the lower minimum value of the height of the available subantral bone for the application of the method.

6. The three-dimensional FDM printed simulation models reproduce the anatomical features in detail and serve as an operating field simulator for the purpose of training the operator's manual skills, the materialized visualization of the surgical field provides an opportunity to find the most accurate approach in the preoperative preparation of a clinical case.

7. For the needs of dental implantology, when carrying out an endoscopically guided maxillary sinus floor augmentation procedure, it is appropriate for the endoscopic approach to be performed through the fossa canina.

8. The largest share of visibility from the total area of observation of the sinus floor is achieved when the endoscope enters in an antero-posterior direction at 10 mm and a degree of observation of 45° at comparable 15°, 45° and 90°.

9. The opening for endoscopic approach made by trocar-guided technique is a difficult task compared to machine osteotomy technique.

10. The trocar-guided technique offers no advantages over the machine osteotomy technique, and endoscope visibility is the same with both techniques for creating an approach opening.

6. CONTRIBUTIONS

Original contributions

1. For the first time, a visibility share of the total observation area of the sinus floor through an endoscope is examined, when entering it in the antero-posterior direction in two positions 10 and 20 mm, observation angle 15°, 45° and 90°, as well as opening for the endoscopic approach through the fossa canina in three directions.

2. For the first time, the trocar-guided technique and the machine osteotomy technique for creating an opening for endoscopic approach are compared.

Affirmative contributions

1. We confirmed that the height of the available subantral bone decreases from the premolar to the molar region, and the width of the available subantral bone and the width of the maxillary sinus increase from the molar to the premolar region.

2. We confirmed a significant inverse relationship between the width of the maxillary sinus and the height of the available subantral bone, and a significant direct relationship was observed between the width of the maxillary sinus and the width of the available subantral bone.

3. We confirmed that the height of available subantral bone at which maxillary sinus floor augmentation with lateral approach with immediate implant placement is undertaken acquires a wider range.

4. We confirmed that the height of the available subantral bone is a factor in undertaking an implant placement method in the setting of subantral deficiency in a maxillary sinus floor augmentation with lateral approach with immediate implant placement.

5. We confirmed that the 3D FDM printed anatomical simulation models can be incorporated into the preoperative preparation and planning of the surgical manipulation, in order to understand the individual anatomy of certain objects, through their visualization, and also serve as a physical object for training in the performance of specific surgical techniques to improve the operator's dexterity.

6. We confirmed that for the needs of dental implantology, when performing an endoscopically guided sinus floor elevation procedure, it is appropriate for the endoscopic approach to be performed through the fossa canina.

7. PUBLICATIONS, RELATED TO THE DISSERTATION

1. *Subantral bone loss specification* - Desislava Stoyanova, Stefan Peev, Nikolay Sapundzhiev, Anjela Bakhova; International Journal of Science and Research (IJSR), Volume 11 Issue 5, May 2022, DOI: 10.21275/SR22502190709, ISSN: 2319-7064(Online)

2. *Endoscopic Access Possibility in Maxillary Sinus Floor Augmentation* - Desislava Stoyanova, Stefan Peev, Nikolay Sapundzhiev, Anjela Bakhova; International Journal of Science and Research (IJSR), Volume 11 Issue 5, May 2022, DOI: 10.21275/SR22518162334, ISSN: 2319-7064(Online)

3. *3D Printed Models Application in Training of Endoscopically Navigated Maxillary Sinus Floor Augmentation Procedure* - Desislava Stoyanova, Stefan Peev, Nikolay Sapundzhiev; International Journal of Science and Research (IJSR), Volume 11 Issue 6, June 2022; DOI: 10.21275/SR22603163022, ISSN: 2319-7064(Online)